NASA TM X-219

TECHNICAL MEMORANDUM
X-219

AERODYNAMIC CHARACTERISTICS OF A 60° SWEPTBACK-WING AIRPLANE CONFIGURATION HAVING TAIL SURFACES LOCATED OUTBOARD OF THE WINGTIPS AT MACH NUMBERS OF 2.30, 2.97, 3.51, AND 4.06

By William C. Sleeman, Jr., James D. Church,
and Roger H. Fournier

Langley Research Center
Langley Field, Va.

[redacted]

NATIONAL AERONAUTICS AND SPACE ADMINISTRATION
WASHINGTON
March 1960

[redacted]

NATIONAL AERONAUTICS AND SPACE ADMINISTRATION

TECHNICAL MEMORANDUM X-219

AERODYNAMIC CHARACTERISTICS OF A 60° SWEPTBACK-WING AIRPLANE CONFIGURATION HAVING TAIL SURFACES LOCATED OUTBOARD OF THE WINGTIPS AT MACH NUMBERS OF 2.30, 2.97, 3.51, AND 4.06*

By William C. Sleeman, Jr., James D. Church, and Roger H. Fournier

SUMMARY

33321

An investigation has been conducted in the Langley Unitary Plan wind tunnel to determine the drag, static longitudinal and lateral stability, and longitudinal trim characteristics of an airplane configuration having tail surfaces located outboard of the wingtips. The trapezoidal wing of the model had 60° sweepback at the leading edge, an aspect ratio of 0.90, and hexagonal airfoil sections $2\frac{1}{2}$ percent chord thick. Longitudinal characteristics were obtained with two sizes of horizontal tails, having areas 20 and 25 percent of the wing area. Data were obtained over an angle-of-attack range from approximately -3° to 13° at Mach numbers of 2.30, 2.97, 3.51, and 4.06 for a Reynolds number of 2.03×10^6.

Author

The maximum value of lift-drag ratio obtained for the basic model with 0° stabilizer setting was approximately 6.3 at a Mach number of 3.51. This value would apply for trimmed conditions with a static margin at low lift of approximately 8 percent mean aerodynamic chord. For a low-lift static margin of 13 percent mean aerodynamic chord, trimmed lift-drag ratios of 6.1 were obtained and were essentially invariant with Mach number from 2.30 to 4.06. However, with the static margin of 13 percent mean aerodynamic chord, static longitudinal instability would be expected for lift coefficients above approximately 0.20. The static directional stability of the complete model was positive for all test conditions except at a Mach number of 4.06 for angles of attack between approximately 11° and 13° where the stability was neutral.

*Title, Unclassified.

INTRODUCTION

The National Aeronautics and Space Administration has been giving considerable attention to the problem of attaining high values of lift-drag ratio for airplane configurations designed to cruise near a Mach number of 3.0. Investigations of several different airplane configurations representing different approaches to the problem are reported in references 1 to 3 and are summarized in reference 4. Results of these investigations demonstrate that fairly high values of lift-drag ratio can be attained near a Mach number of 3.0 for trimmed conditions.

The present study and that of reference 5 were undertaken as a further investigation of the type of outboard-tail configuration reported in reference 1 with the purpose of obtaining improvements in performance and stability by means of geometric modifications suggested, in part, by the experimental results of references 1 and 6. These changes in geometry were so extensive that the present model was a completely different outboard-tail configuration and could not be considered a modification of the first outboard-tail model (ref. 1). Most of the changes made were directed toward reducing the minimum drag and included reducing the ratio of volume to wing area by reducing the wing thickness-chord ratio and reducing the volume of both the fuselage and wingtip bodies. Other changes included reduction in wing sweep and aspect ratio, reduction in the ratio of tail area to wing area, increase in the relative size of the engine pack, and addition of wing trailing-edge extensions. In order to expedite construction, the present model was simplified by eliminating the wing twist and dihedral used in the model of reference 1. However, the analysis presented in reference 7 of estimated lateral dynamic characteristics indicated that a very small value of effective dihedral as obtained with the model of reference 1 is favorable (negative geometric dihedral will offset the positive dihedral effect of the lifting wing) for design conditions near a Mach number of 3.0. Therefore, the use of negative geometric dihedral on the present model would have been desirable to offset the large positive dihedral effect at lifting conditions.

The present tests were conducted at the Langley Unitary Plan wind tunnel at Mach numbers of 2.30, 2.97, 3.51, and 4.06 at a Reynolds number of 2.03×10^6 for an angle-of-attack range from approximately -3° to 13°. Longitudinal characteristics were obtained with horizontal tails of two different sizes, the basic tail surfaces (used on the configuration referred to as the basic model) had an area of 20 percent of the wing area and the large tail surfaces had an area of 25 percent of the wing area. Lateral stability derivatives for the basic model were obtained from tests through the angle-of-attack range at fixed sideslip angles of $\pm 4^\circ$. Data were also obtained over a range of sideslip angles from -4° to 10° for angles of attack of approximately 4° and 8° at a Mach number of 2.97. A summary of the results of this investigation is

presented; however discussion and analysis of the data have been omitted in order to expedite publication of these data.

SYMBOLS

The data of this investigation are referred to the system of axes shown in figure 1. The lateral characteristics are referred to the body axes and the longitudinal characteristics are referred to the stability axes. Moment coefficients are given about a moment reference located at 50.12 percent of the mean aerodynamic chord of the wing alone (excluding the tail surfaces).

C_L lift coefficient, $\frac{\text{Lift}}{qS}$

C_D external-flow drag coefficient, $\frac{\text{Total drag}}{qS} - \left(C_{D,b} + C_{D,i}\right)$

$C_{D,b}$ base-pressure drag coefficient

$C_{D,i}$ engine-pack internal-flow drag coefficient

C_m pitching-moment coefficient, $\frac{\text{Pitching moment}}{qS\bar{c}}$

C_l rolling-moment coefficient, $\frac{\text{Rolling moment}}{qSb}$

C_n yawing-moment coefficient, $\frac{\text{Yawing moment}}{qSb}$

C_Y side-force coefficient, $\frac{\text{Side force}}{qS}$

C_{l_β} effective dihedral parameter, $\left(\frac{\Delta C_l}{\Delta \beta}\right)_{\beta=\pm 4^\circ}$

C_{n_β} directional-stability parameter, $\left(\frac{\Delta C_n}{\Delta \beta}\right)_{\beta=\pm 4^\circ}$

C_{Y_β} side-force parameter, $\left(\frac{\Delta C_Y}{\Delta \beta}\right)_{\beta=\pm 4^\circ}$

b	span of wing plus horizontal tail
c	chord of wing or tail
$\bar{c}$	mean aerodynamic chord of wing plus horizontal tail
L/D	lift-drag ratio
M	free-stream Mach number
p_t	free-stream stagnation pressure, lb/sq ft abs
q	free-stream dynamic pressure, lb/sq ft
R	Reynolds number based on $\bar{c}$ of model with basic horizontal tail
S	area of wing plus horizontal tail, including wing-body intercept (wingtip and tail-root chords are assumed to lie on center line of wingtip bodies) but not including area of trailing-edge extensions
α	angle of attack referred to fuselage reference line, deg
β	angle of sideslip referred to fuselage center line, deg
δ_r	rudder deflection relative to chord plane of vertical tail (positive when trailing edge is deflected to left), deg
i_t	horizontal-tail incidence angle relative to center line of rear half of wingtip bodies (positive when trailing edge is down), deg
ϵ	angle of effective downwash at horizontal tail (positive when flow is directed down relative to free stream), deg

Subscripts:

max	maximum
min	minimum

APPARATUS AND MODEL

The tests were conducted in the high Mach number test section of the Langley Unitary Plan wind tunnel. This tunnel is of the variable-pressure, continuous-flow type with a test section 4 feet square and approximately 7 feet in length. The Mach number was varied from 2.30 to 4.06 by means of an asymmetric sliding-block nozzle.

The general arrangement of the outboard-tail model and its engine pack are shown in figure 2 and tabulated geometric characteristics are given in table I. Photographs of the model are shown in figure 3. The wing of the model had 60° sweepback at the leading edge, an aspect ratio of 0.90, and $2\frac{1}{2}$-percent-chord-thick hexagonal airfoil sections with ridge lines at the 1/3- and 2/3-chord lines. The wing was not twisted and had no dihedral or incidence.

The forward part of the fuselage of the model had a cross-sectional shape composed of two semiellipses having their major axes horizontal and coincident. The minor axes of these semiellipses were selected so that the height of the body was one-half of the width. Most of the rear part of the body was a basic semicircular shape with the diameter located on the bottom surface of the wing.

A slender body was affixed to each wingtip and had a 1.2 to 1.0 elliptical cross section with the major axis vertical. The center line of the forward half of the wingtip bodies was parallel to the wing-chord plane, whereas the center line of the rear half was inclined upward 3°. (See fig. 2(a).) The wingtip bodies were "bent" in order to have the horizontal tail sections alined with the bodies at the trim setting for design conditions when used on the present untwisted wing. The wingtip bodies were also "bent" inward at the rear so that the vertical tail surfaces which were alined with the wingtip bodies would have 1.5° of toe-out. (See plan view, fig. 2(a).)

Details of the geometry of the horizontal and vertical tail surfaces are given in table I and figure 2. These surfaces were considered to be undeflected when they were alined with the center lines of the rear part of the wingtip bodies. The wing trailing-edge extension shown in figure 2 extended rearward from the wing trailing edge at approximately the 3° inclination of the rear part of the wingtip body. (See fig. 3.) The total exposed plan-form area of these trailing-edge extensions was 0.115 sq ft; however this added area was not considered in the reference area used in reduction of the present data. Details of the engine pack tested as a part of the basic model are given in figure 2(c). The engine pack consisted of a two-dimensional split inlet that was ducted to exhaust through four choked nozzles. A wedge-type boundary-layer diverter located

on the upper surface of the inlet-duct housing was an integral part of the engine pack.

Forces and moments acting on the model were measured by means of a six-component internal strain-gage balance. This balance was attached, by means of a sting, to the tunnel central support system. A remotely operated, adjustable angle coupling was included in the model support system and this coupling permitted tests to be made at various angles of attack simultaneously with variations in the angle of sideslip.

TESTS

Tests were conducted for all configurations through an angle-of-attack range of approximately -3° to 13° at an angle of sideslip of 0°. Longitudinal characteristics of the basic model were obtained for the complete range of available horizontal-tail settings and with the horizontal tails removed for Mach numbers of 2.30, 2.97, and 3.51. Only limited data were obtained at $M = 4.06$ for some of the configurations. The vertical tail was on the model in a toe-out position for all tests except where the tail was removed to determine the effect on lateral derivatives. The strain-gage balance was mounted in the engine pack and therefore all tests were made with the engine pack on the model.

Average Mach numbers, stagnation pressures, dynamic pressures, and Reynolds number are listed in the following table:

M	p_t, lb/sq ft abs	q, lb/sq ft	R (based on $\bar{c}$)
2.30	1,131	335	2.03×10^6
2.97	1,614	284	2.03
3.51	2,150	240	2.03
4.06	3,007	211	2.03

Stagnation temperature was maintained at 155° F for all Mach numbers.

Pressure measurements were recorded during one of the tests in order to obtain the drag increments associated with base pressure and the engine-pack internal flow. Data were also obtained at $M = 2.97$ with the model at 0° angle of attack for a range of elevated stagnation pressures in order to study the effect of Reynolds number on minimum drag. This test was conducted near zero lift over a Reynolds number range of 2.03×10^6 to 8.88×10^6 based on $\bar{c}$.

Transition was fixed on all configurations by means of roughness strips placed around the fuselage and wingtip bodies about 2 inches behind the noses and along the 5-percent-chord lines (upper and lower surfaces) of the wing and tail surfaces. The transition strips were formed by placing single grains of sand having a nominal size of 0.018 inch along the transition line at a spacing of approximately 1/32 inch between grains.

CORRECTIONS AND ACCURACY

Tunnel pressure gradients in the region of the model have been found to be sufficiently small so as not to induce any measurable buoyancy effects on the model. Corrections for tunnel-airflow misalinement have been determined from tests of the model at erect and inverted positions and these corrections have been applied to the model angle of attack. In addition, all angles of attack and sideslip have been corrected for deflection of the balance-sting combination due to load.

All drag data have been adjusted to correspond to free-stream static pressure acting on the entire base area of the model including the area occupied by the sting but not including the duct exit areas. Pressures measured in the balance chamber and over the engine-pack base were used to obtain base-pressure corrections and were applied to the appropriate areas. A correction for $C_{D,i}$ (force computed from duct and exit pressures by using standard momentum-balance equation) has been subtracted from the measured drag data. The necessary pressure measurements were not made at $M = 4.06$ to obtain $C_{D,i}$ and $C_{D,b}$; consequently extrapolations of these corrections were employed (see fig. 5) in computing the data at this Mach number.

Results of the tests with the large horizontal tail on the model were obtained subsequent to the original tests with the basic horizontal tail, and different strain-gage balances were used. The balance employed in tests of the model with the basic horizontal tail and in tests with the tail off is designated balance A, and the balance used with the large horizontal tail is designated balance B. Accuracy of the presented data based on design specifications for the strain-gage balance and tunnel calibration is estimated to be within the following limits:

M	± 0.015
α, deg	± 0.2
β, deg	± 0.2
i_t, deg	± 0.1
δ_r, deg	± 0.1

	Balance A	Balance B
C_L	±0.003	±0.001
C_D	±0.0006	±0.0005
C_m	±0.002	±0.002
C_l	±0.0003	±0.0002
C_n	±0.0008	±0.0006
C_Y	±0.002	±0.003

In some cases, because of normal-force zero shifts induced by temperature effects in balance A, the limits in values for C_L, C_D, and C_m are somewhat greater than those given in the table. The stated accuracy limits for balance B are believed to apply for all the present tests with this balance.

PRESENTATION OF RESULTS

The basic results of this investigation are presented in figures 4 to 13 and some results are summarized in figures 14 to 17. An outline of the figure content is as follows:

	Figure
Schlieren photographs	4
Internal-flow and base-pressure drag coefficients	5
Effect of Reynolds number on minimum drag coefficient	6
Longitudinal characteristics:	
Basic tail	7
Large tail	8, 9
Use of horizontal tail as a roll control	10
Effect of rudder deflection	11
Lateral stability derivatives	12
Aerodynamic characteristics in sideslip	13
Summary of longitudinal stability parameters	14
Summary of performance parameters	15
Effect of stability on trimmed lift-drag ratios	16
Comparison of performance parameters for basic model with those for model of reference 1	17

SUMMARY OF RESULTS

The main results of an investigation at Mach numbers of 2.30, 2.97, 3.51, and 4.06 of an outboard-tail airplane configuration having a 60° sweptback wing may be summarized as follows:

The maximum value of lift-drag ratio obtained for the basic model with $i_t = 0°$ (fig. 15) was approximately 6.3 at a Mach number of 3.51. This value would apply for trimmed conditions with a static margin at low lift of approximately 8 percent mean aerodynamic chord. For a low-lift static margin of approximately 13 percent mean aerodynamic chord, trimmed lift-drag ratios of 6.1 were obtained and were essentially invariant with Mach number from 2.30 to 4.06 (fig. 16). However, with the static margin of 13 percent mean aerodynamic chord, static longitudinal instability would be expected for lift coefficients above approximately 0.20 (fig. 7).

A comparison of maximum lift-drag ratios for the present basic model with those for the outboard-tail model of reference 1 shows opposite trends with increasing Mach number from 2.30 to 3.51 (fig. 17). The model of reference 1 had a maximum lift-drag ratio of 6.4 at a Mach number of 2.30 which decreased to a value of 5.5 at a Mach number of 3.51, whereas for the same Mach numbers, maximum lift-drag ratios of the present basic model increased from 6.1 to 6.3. In comparison with the model of reference 1, the refinements incorporated in the present model, such as thinner airfoil sections, more slender fuselage and wing-tip bodies, and slightly lower volume-to-wing-area ratio, would be expected to result in improvements in lift-drag ratio throughout the Mach number range. Reasons why these expected improvements were not realized at the lower Mach numbers are not readily apparent; however there is evidence that for the present model, appreciable external spillage from the inlet was present near a Mach number of 2. This external flow would cause a drag increment which did not appear in the internal-flow measurements and which would be expected to materially diminish as the test Mach number approached the inlet design Mach number of 3.0.

The static directional stability of the complete model was positive for all test conditions except at a Mach number of 4.06 for angles of attack between approximately 11° and 13° where the directional stability was neutral. Positive effective dihedral at positive lift coefficients was indicated for all test conditions.

Langley Research Center,
National Aeronautics and Space Administration,
Langley Field, Va., October 14, 1959.

REFERENCES

1. Church, James D., Hayes, William C., Jr., and Sleeman, William C., Jr.: Investigation of Aerodynamic Characteristics of an Airplane Configuration Having Tail Surfaces Outboard of the Wing Tips at Mach Numbers of 2.30, 2.97, and 3.51. NACA RM L58C25, 1958.

2. Kelly, Thomas C., Carmel, Melvin M., and Gregory, Donald T.: An Exploratory Investigation at Mach Numbers of 2.50 and 2.87 of a Canard Bomber-Type Configuration Designed for Supersonic Cruise Flight. NACA RM L58B28, 1958.

3. Hallissy, Joseph M., Jr., and Hasson, Dennis F.: Aerodynamic Characteristics at Mach Numbers 2.36 and 2.87 of an Airplane Configuration Having a Cambered Arrow Wing With a 75° Swept Leading Edge. NACA RM L58E21, 1958.

4. Baals, Donald D., Toll, Thomas A., and Morris, Owen G.: Airplane Configurations for Cruise at a Mach Number of 3. NACA RM L58E14a, 1958.

5. Driver, Cornelius, and Spearman, M. Leroy: Static Stability and Control Characteristics of an Airplane Model With Tail Surfaces Outboard of the Wing Tips at a Mach Number of 2.01. NASA TM X-47, 1959.

6. Hayes, William C., Jr., and Sleeman, William C., Jr.: Low-Speed Investigation of the Effects of Horizontal-Tail Area and Wing Sweep on the Static Longitudinal Stability and Control Characteristics of an Airplane Configuration Having Tail Surfaces Outboard of the Wing Tips. NASA MEMO 6-11-59L, 1959.

7. Sherman, Windsor L.: A Theoretical Investigation of the Dynamic Lateral Stability of Three Possible Airplane Configurations for Flight at a Mach Number of 3.0. NASA MEMO 5-15-59L, 1959.

TABLE I.- GEOMETRIC CHARACTERISTICS OF MODEL

Wing plus basic horizontal tail (used in reduction of all data except data for model with large horizontal tail):	
Area, sq ft	2.5000
Span, ft	2.2941
Mean aerodynamic chord, ft	1.3690
Aspect ratio	2.1052
Taper ratio	0.0986
Wing plus large horizontal tail (used in reduction of data obtained with large horizontal tail):	
Area, sq ft	2.6041
Span, ft	2.4096
Mean aerodynamic chord, ft	1.3457
Aspect ratio	2.2296
Taper ratio	0.1096
Wing:	
Area, sq ft	2.0833
Span, ft	1.3693
Mean aerodynamic chord, ft	1.5419
Aspect ratio	0.9000
Taper ratio	0.6654
Twist, deg	0
Dihedral, deg	0
Leading-edge sweepback, deg	60.00
Trailing-edge sweepback, deg	40.00
Exposed volume, cu ft	0.04021
Airfoil section	$2\frac{1}{2}$ percent thick, hexagonal
Basic horizontal tail (panel geometry):	
Area, sq ft	0.2083
Span, ft	0.4624
Mean aerodynamic chord, ft	0.5046
Aspect ratio	1.0392
Taper ratio	0.2500
Leading-edge sweepback, deg	61.50
Trailing-edge sweepback, deg	30.88
Exposed volume, cu ft	0.00187
Airfoil section	$2\frac{1}{2}$ percent thick, hexagonal

[redacted]

TABLE I.- GEOMETRIC CHARACTERISTICS OF MODEL - Concluded

Large horizontal tail (panel geometry):	
Area, sq ft	0.2604
Span, ft	0.5202
Mean aerodynamic chord, ft	0.5606
Aspect ratio	1.0392
Taper ratio	0.2500
Leading-edge sweepback, deg	61.50
Trailing-edge sweepback, deg	31.50
Exposed volume, cu ft	0.00244
Airfoil section	$2\frac{1}{2}$ percent thick, hexagonal
Vertical tail (panel geometry):	
Area, sq ft	0.1389
Span, ft	0.3223
Mean aerodynamic chord	0.4826
Aspect ratio	0.7479
Taper ratio	0.2500
Incidence (toe-out), deg	1.50
Rudder area, sq ft	0.0463
Location of rudder hinge line, percent chord	66.67
Leading-edge sweepback, deg	52.00
Trailing-edge sweepback, deg	-13.00
Exposed volume, cu ft	0.00095
Airfoil section	$2\frac{1}{2}$ percent thick, double wedge
Wingtip bodies:	
Length, ft	2.2917
Fineness ratio	20.14
Volume, cu ft (each)	0.01045
Fuselage:	
Length, ft	3.2917
Fineness ratio	15.65
Volume, cu ft	0.06294
Engine pack:	
Base area, sq ft (excluding four exits and cavity area)	0.0228
Cavity area, sq ft	0.0167
Capture area, sq ft	0.0309
Enclosed volume, cu ft	0.05941

L 4 6 9

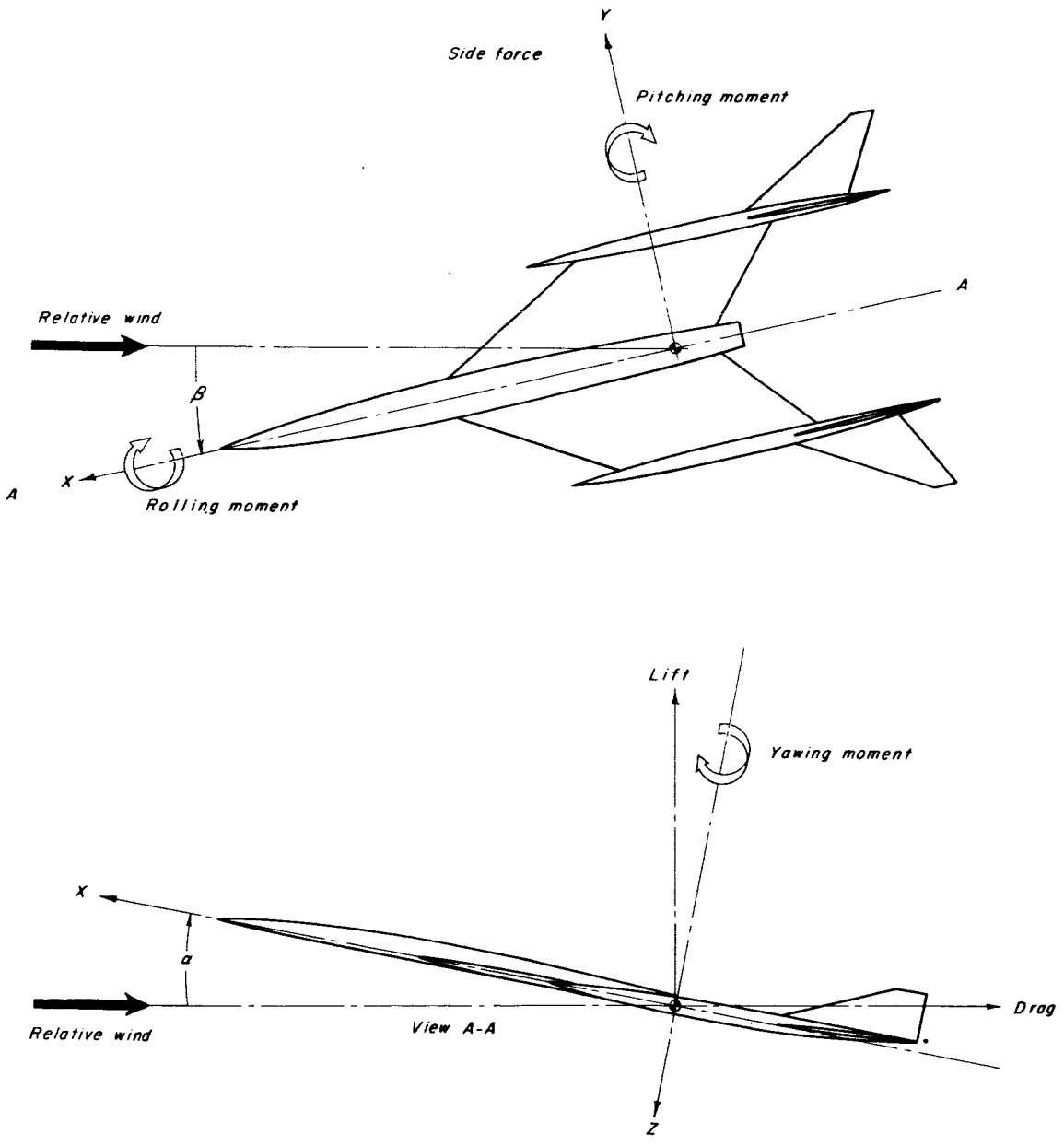

Figure 1.- System of axes used in presentation of data.

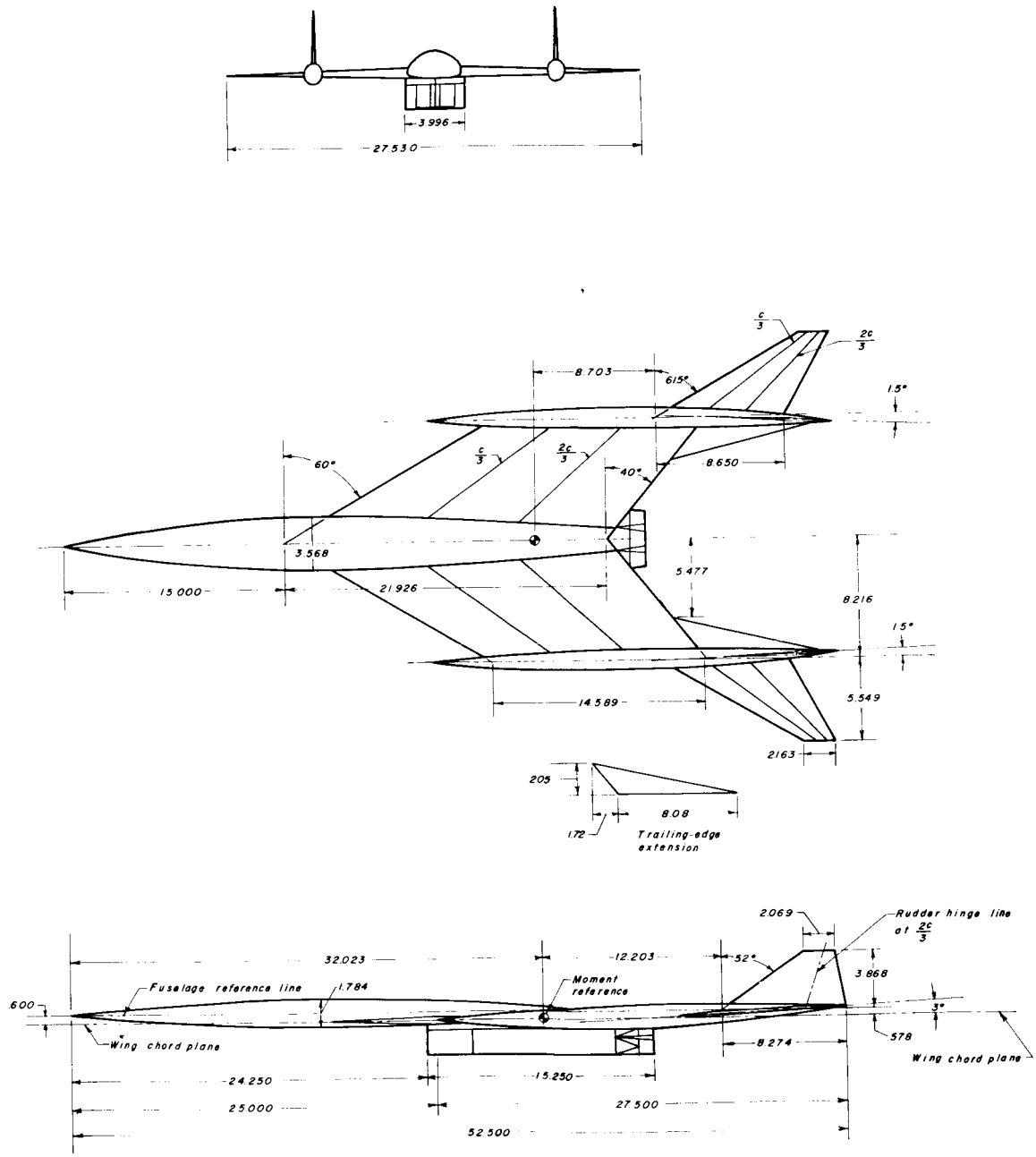

(a) Three-view drawing of basic model.

Figure 2.- General arrangement of outboard-tail model. All dimensions are in inches.

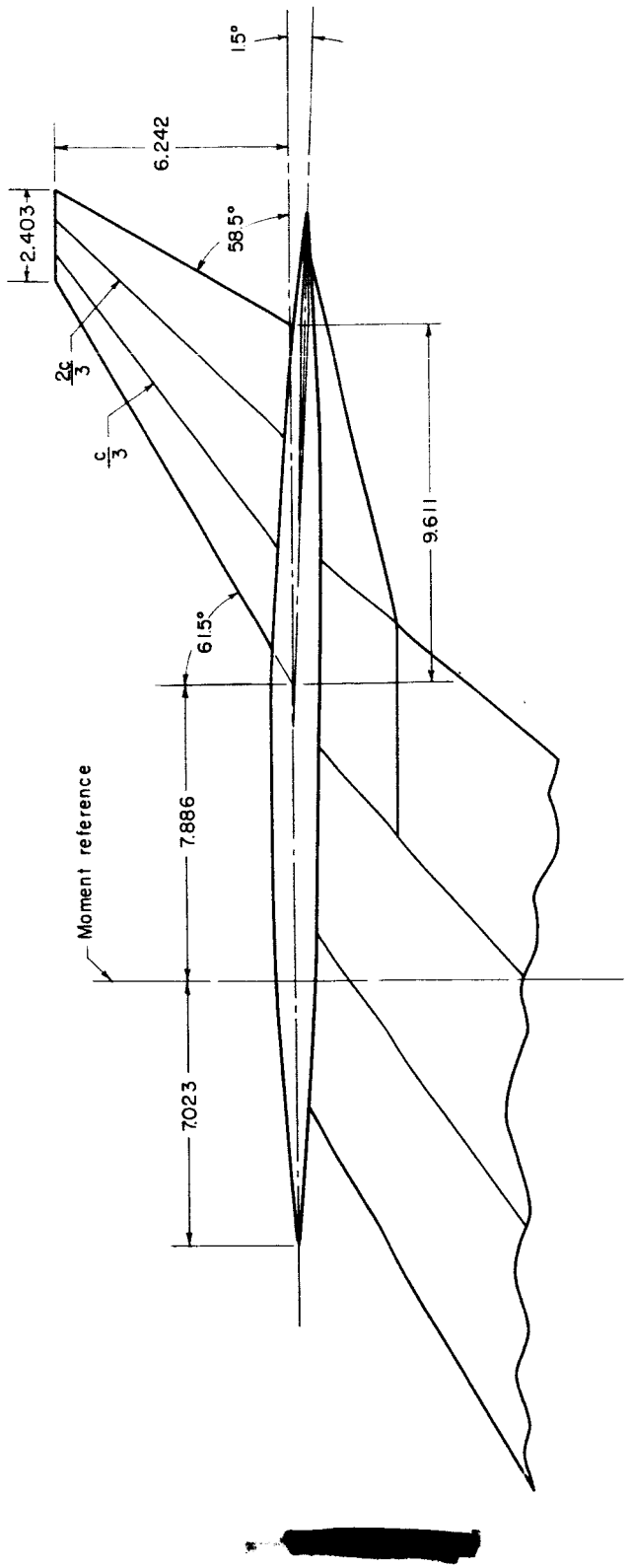

(b) Details of large horizontal tail.

Figure 2.- Continued.

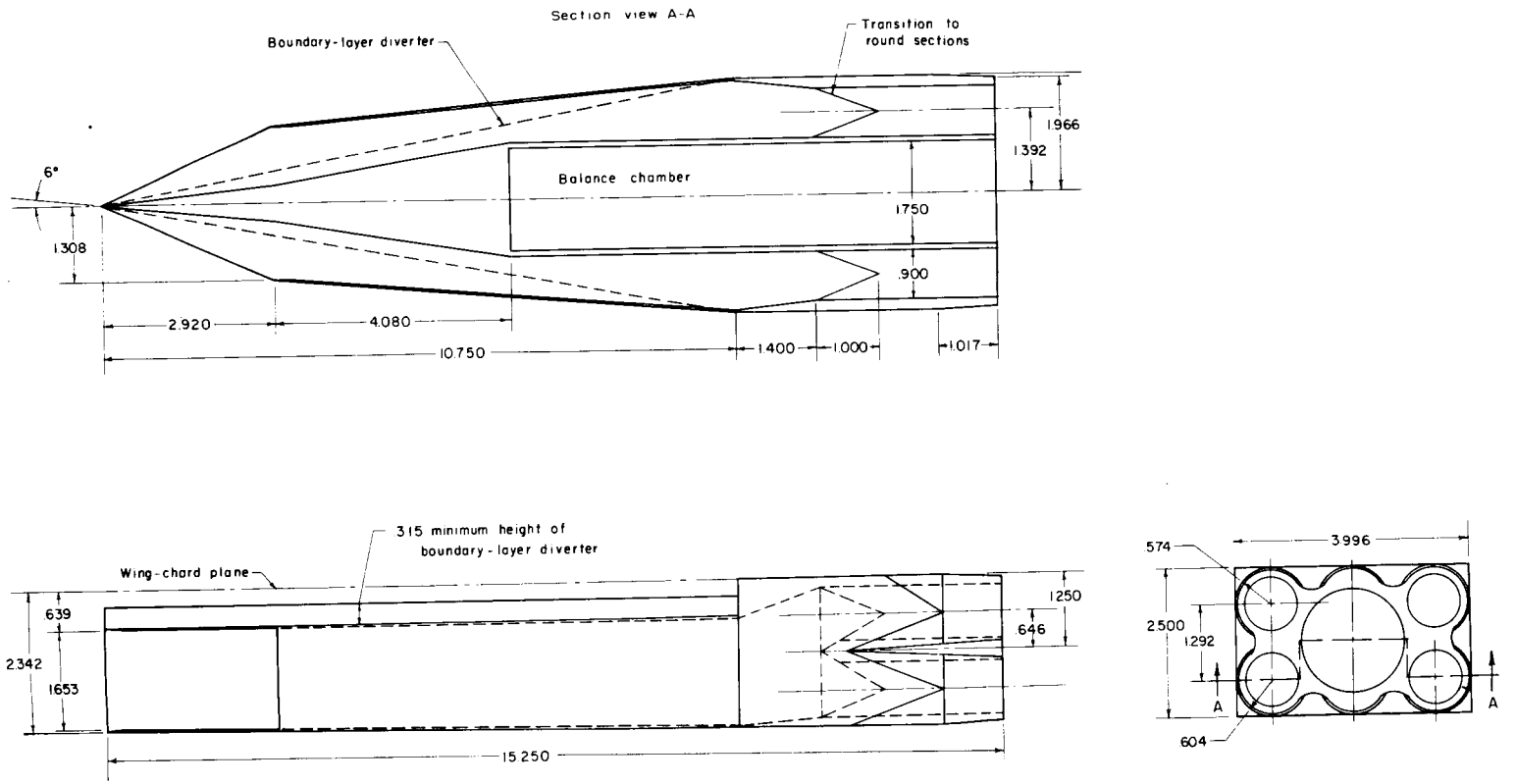

(c) Details of engine pack.

Figure 2.- Concluded.

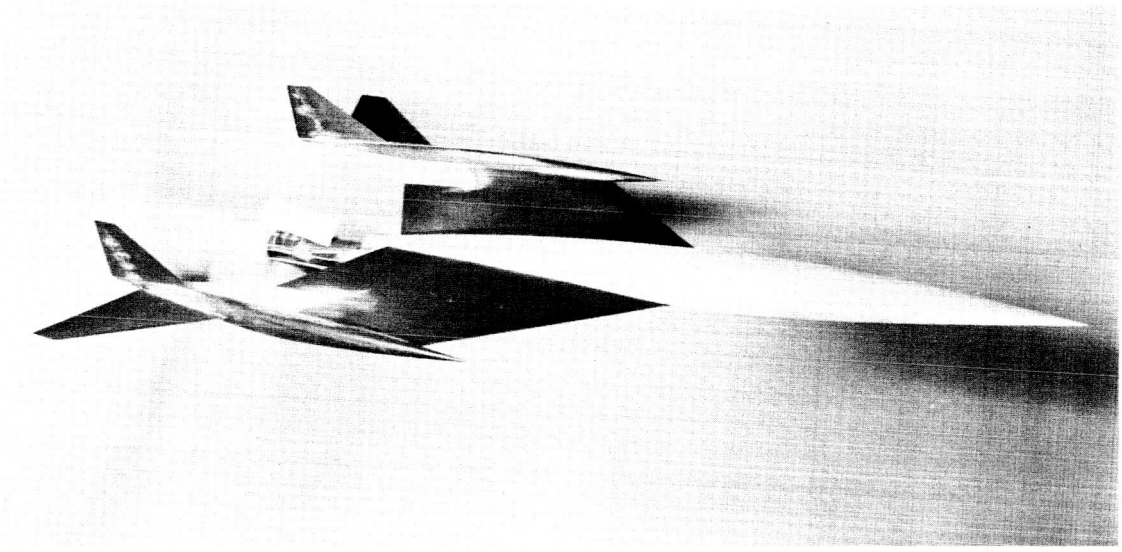

L-58-2295

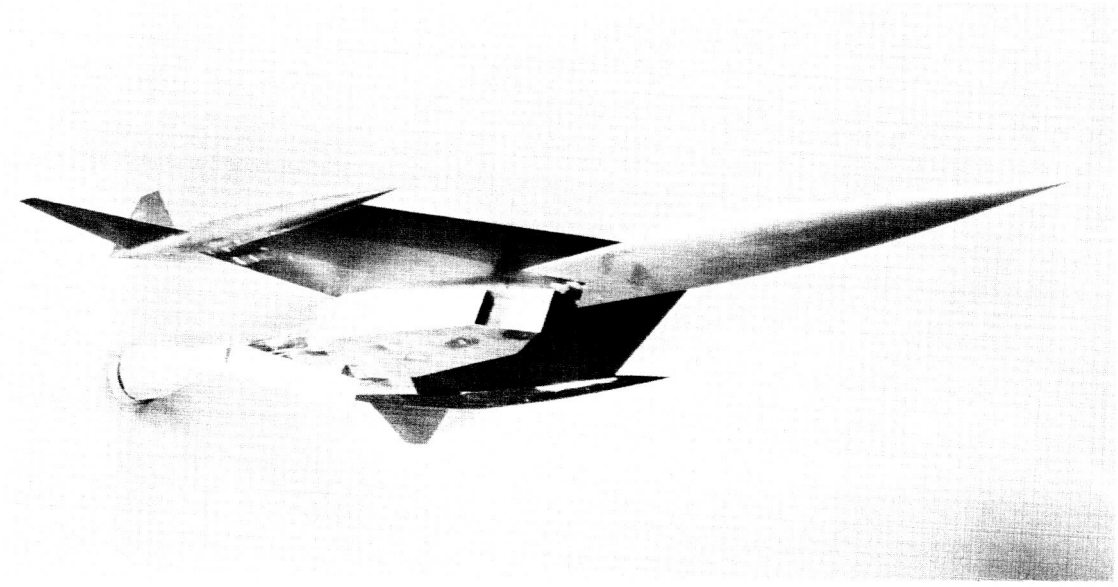

Figure 3.- Photographs of the basic model. L-58-2297

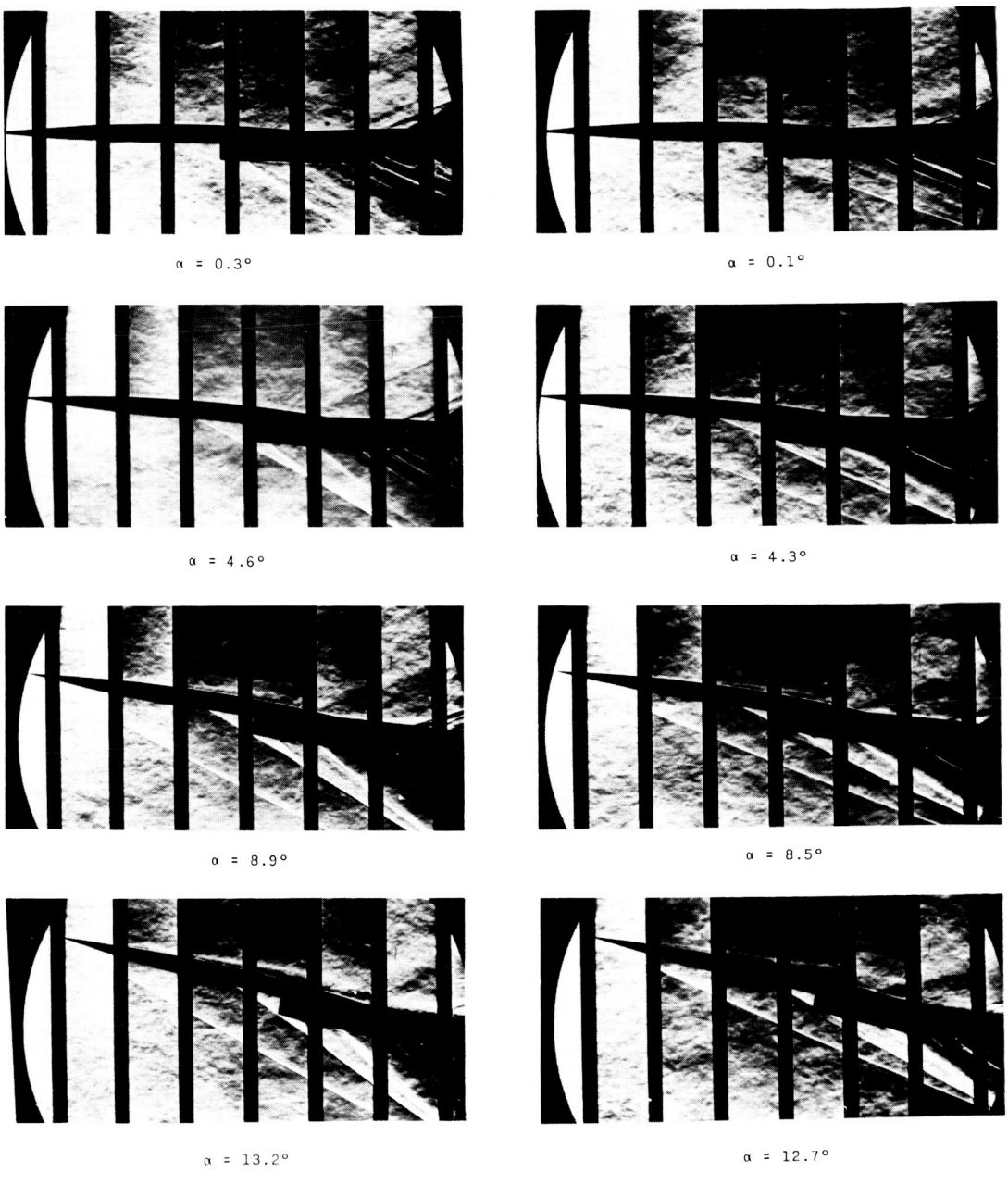

(a) M = 2.30. (b) M = 2.97.

Figure 4.- Typical schlieren photographs. L-59-6094

α = 0°

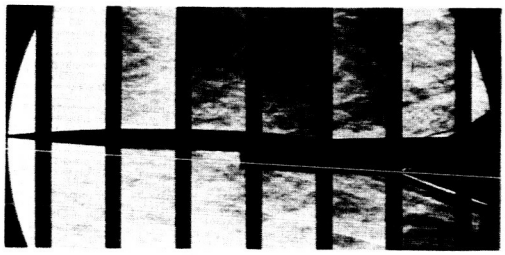

α = 0.4°

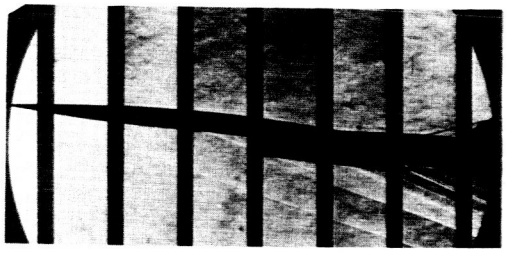

α = 4.1°

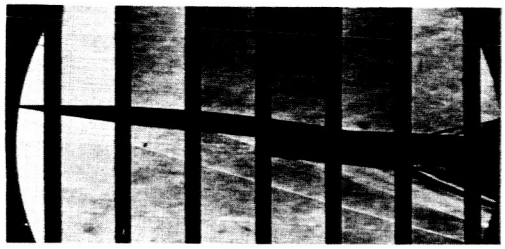

α = 4.6°

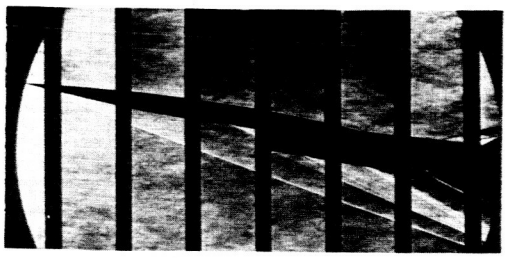

α = 8.3°

α = 8.7°

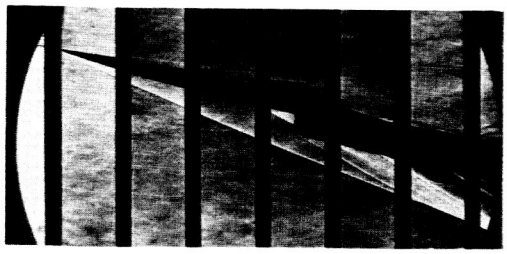

α = 12.5°

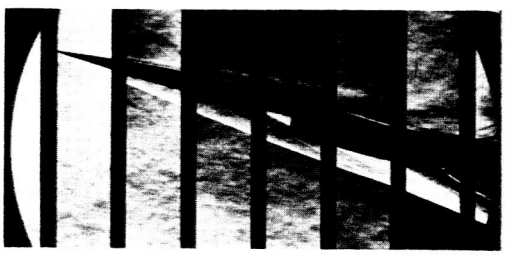

α = 12.8°

(c) M = 3.51.

(d) M = 4.06.

Figure 4.- Concluded. L-59-6095

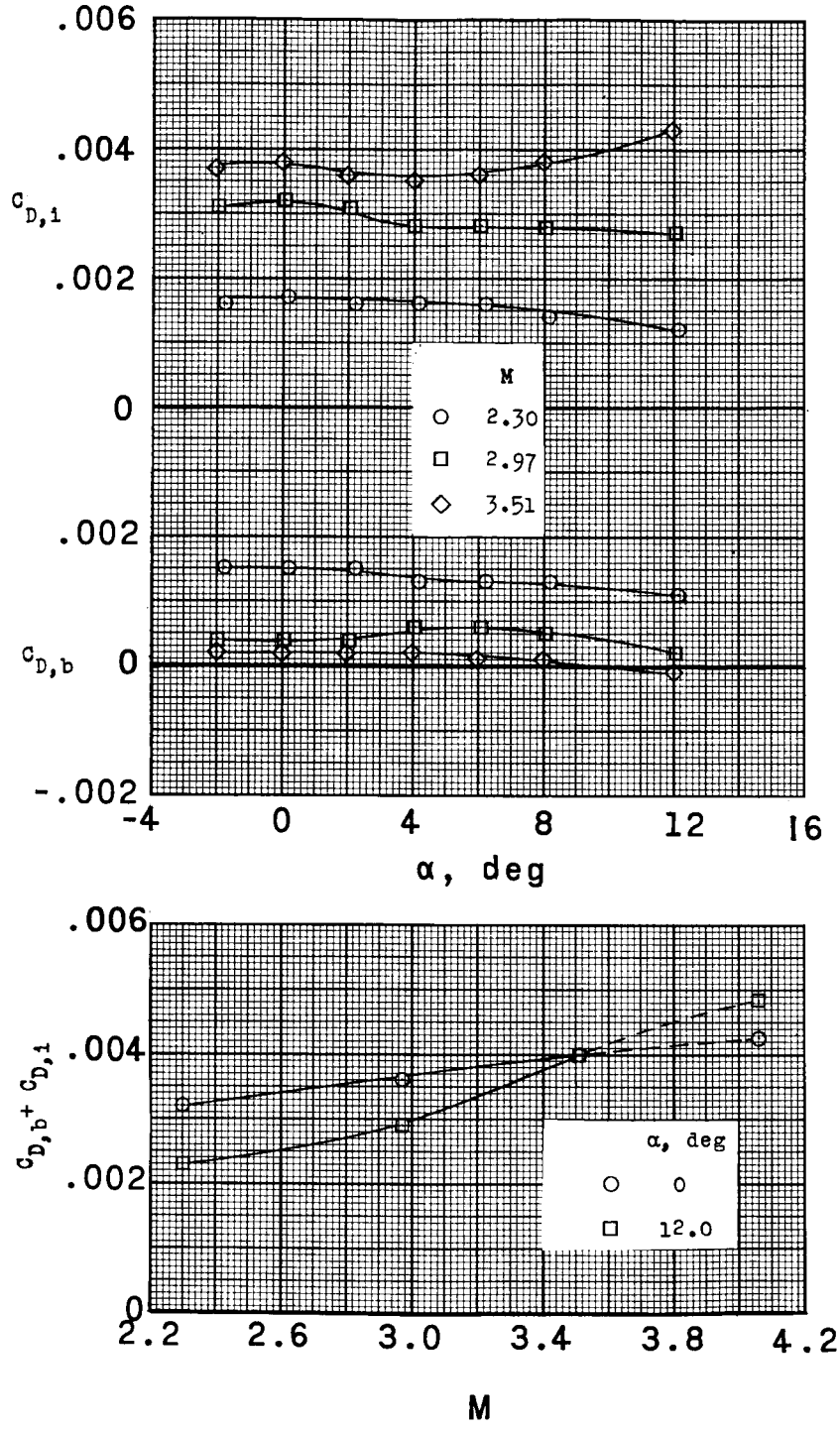

Figure 5.- Variation of internal-flow and base-pressure drag coefficients with angle of attack and Mach number.

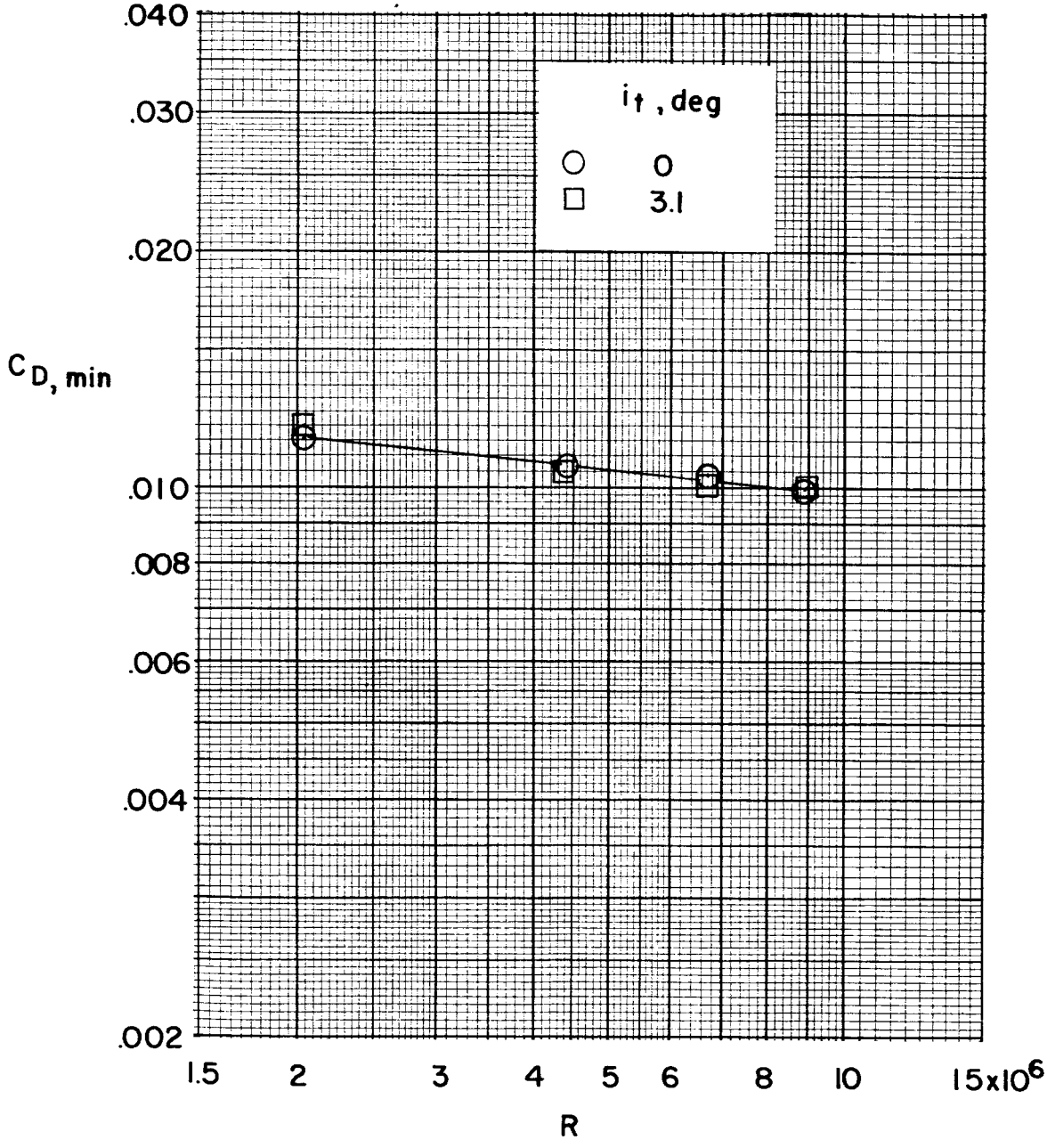

Figure 6.- Variation of minimum drag coefficient with Reynolds number (based on $\bar{c}$) for the basic model at M = 2.97.

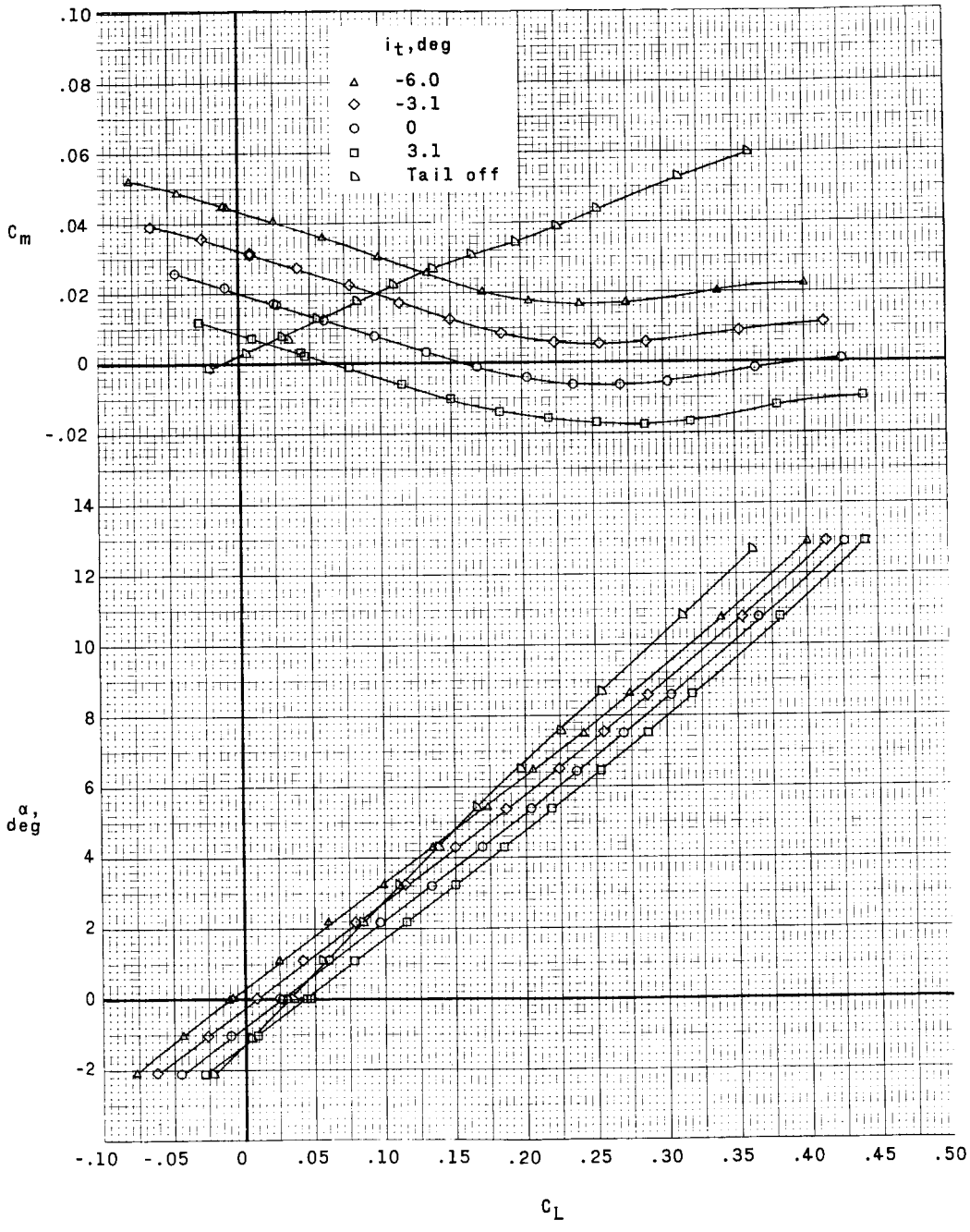

(a) M = 2.30.

Figure 7.- Effect of the basic horizontal tail and tail incidence on aerodynamic characteristics in pitch of the model.

L-469

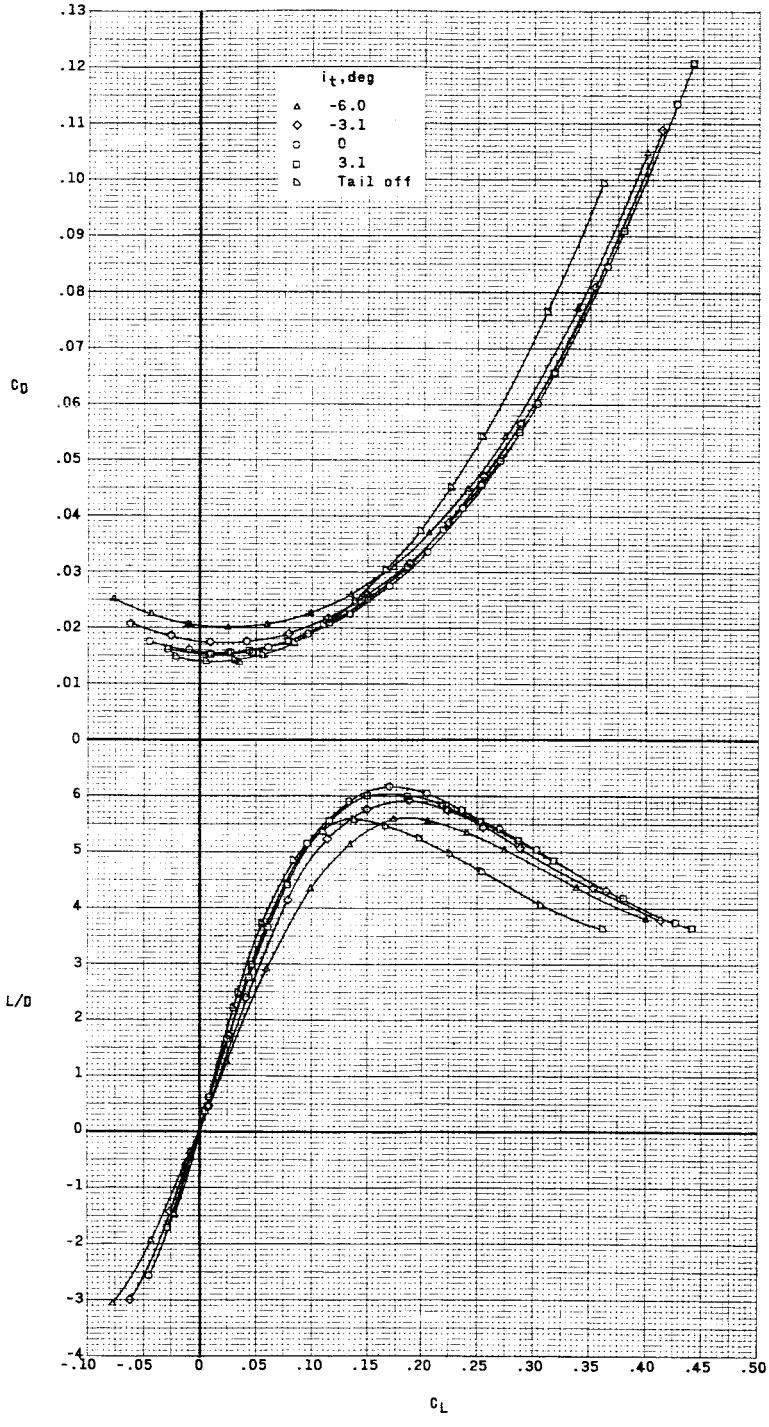

(a) M = 2.30. Concluded.

Figure 7.- Continued.

L-469

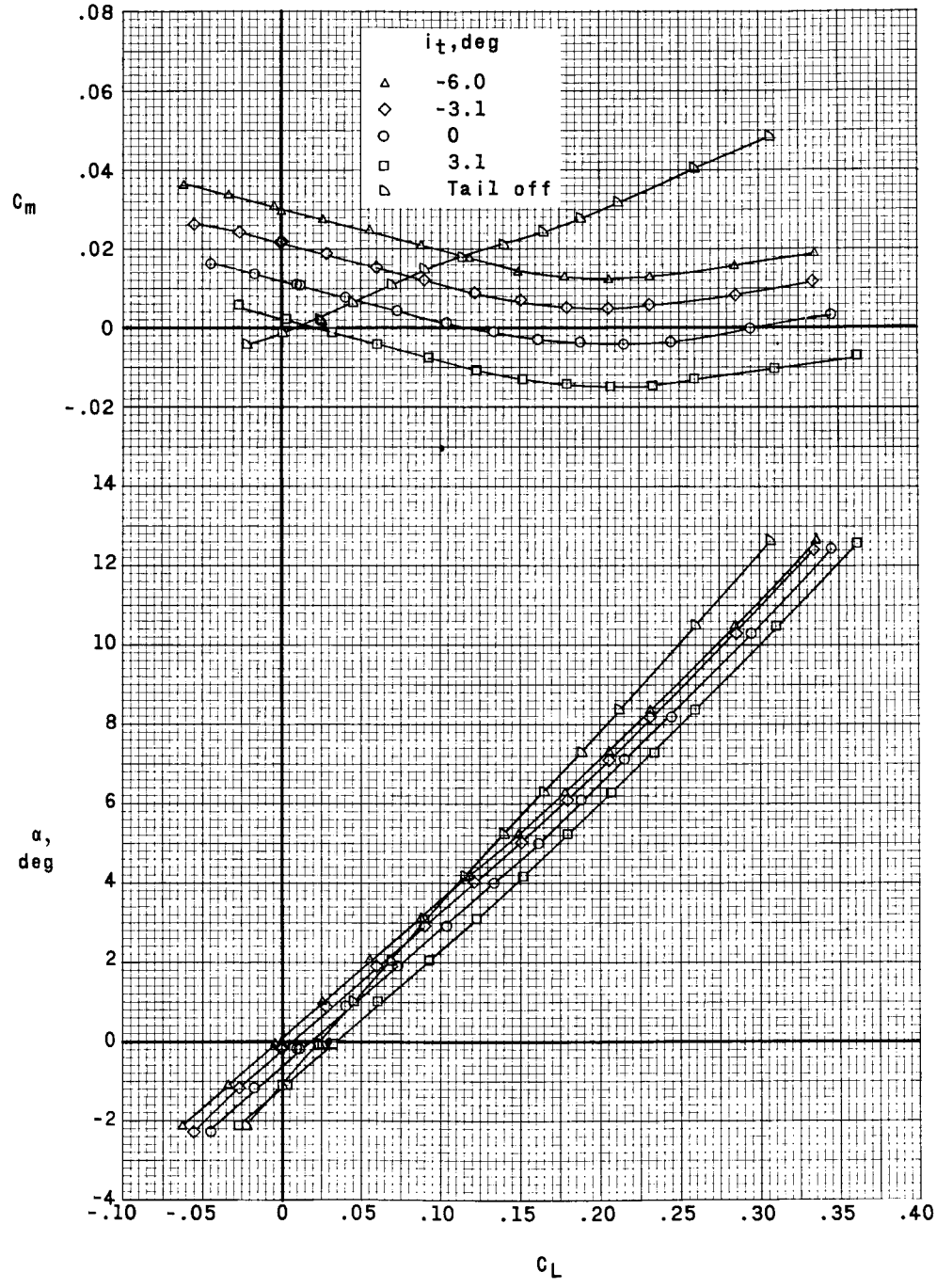

(b) M = 2.97.

Figure 7.- Continued.

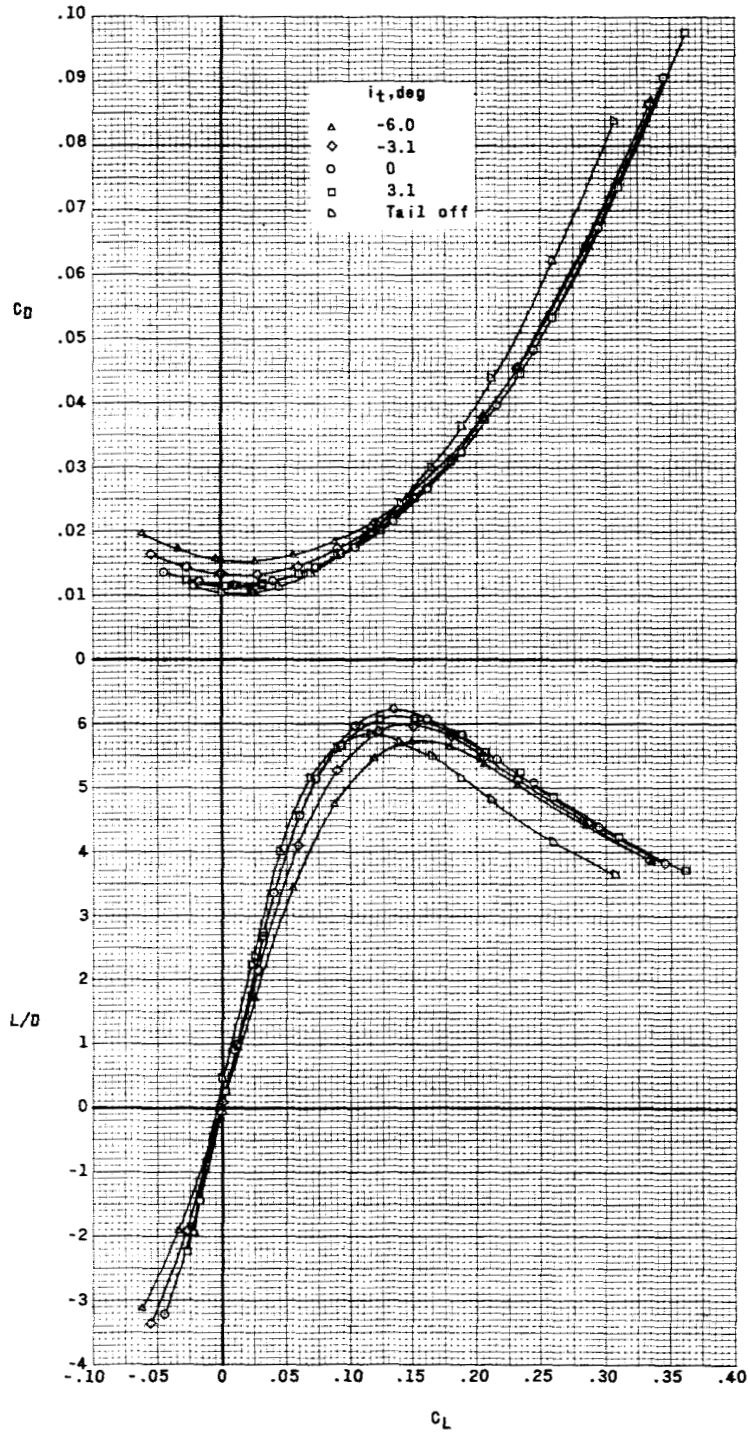

(b) M = 2.97. Concluded.

Figure 7.- Continued.

[redacted]

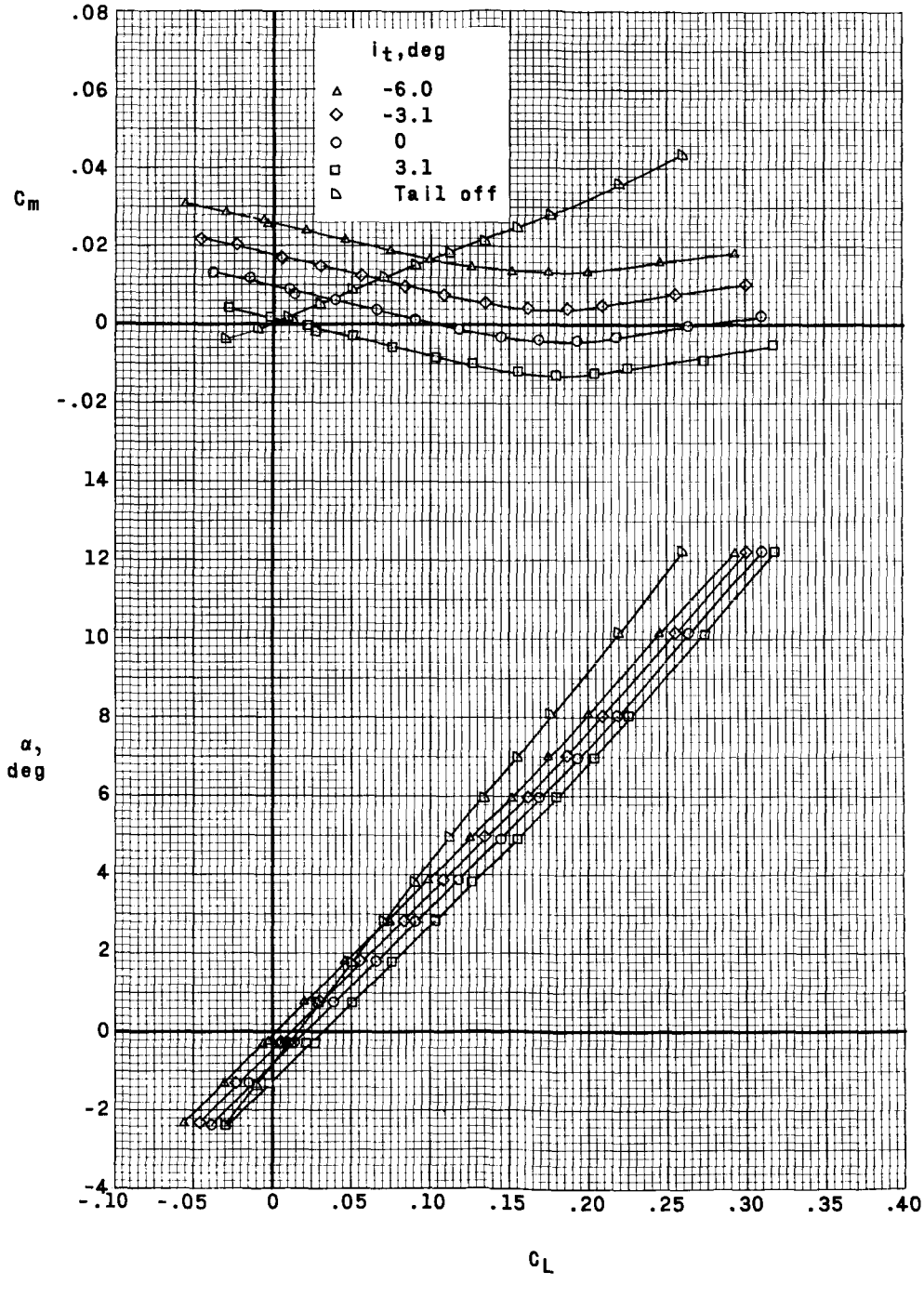

(c) M = 3.51.

Figure 7.- Continued.

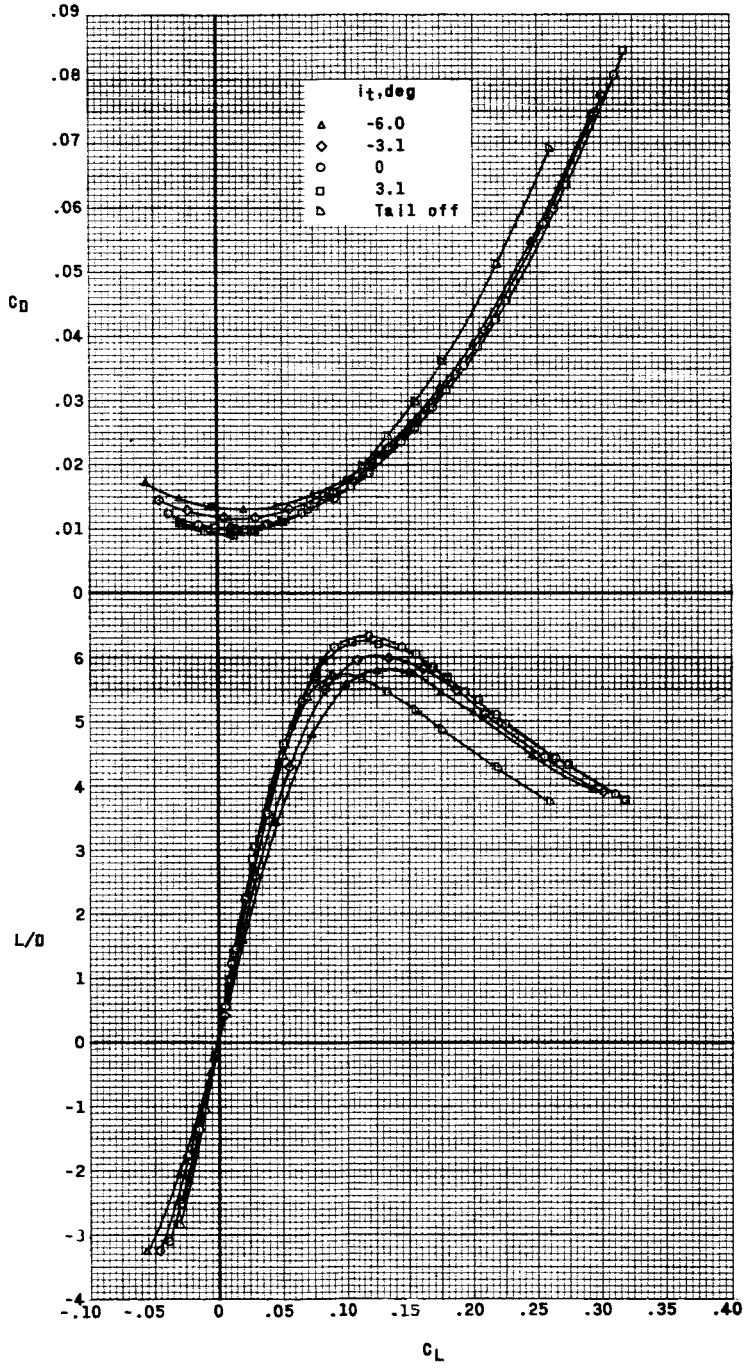

(c) M = 3.51. Concluded.

Figure 7.- Continued.

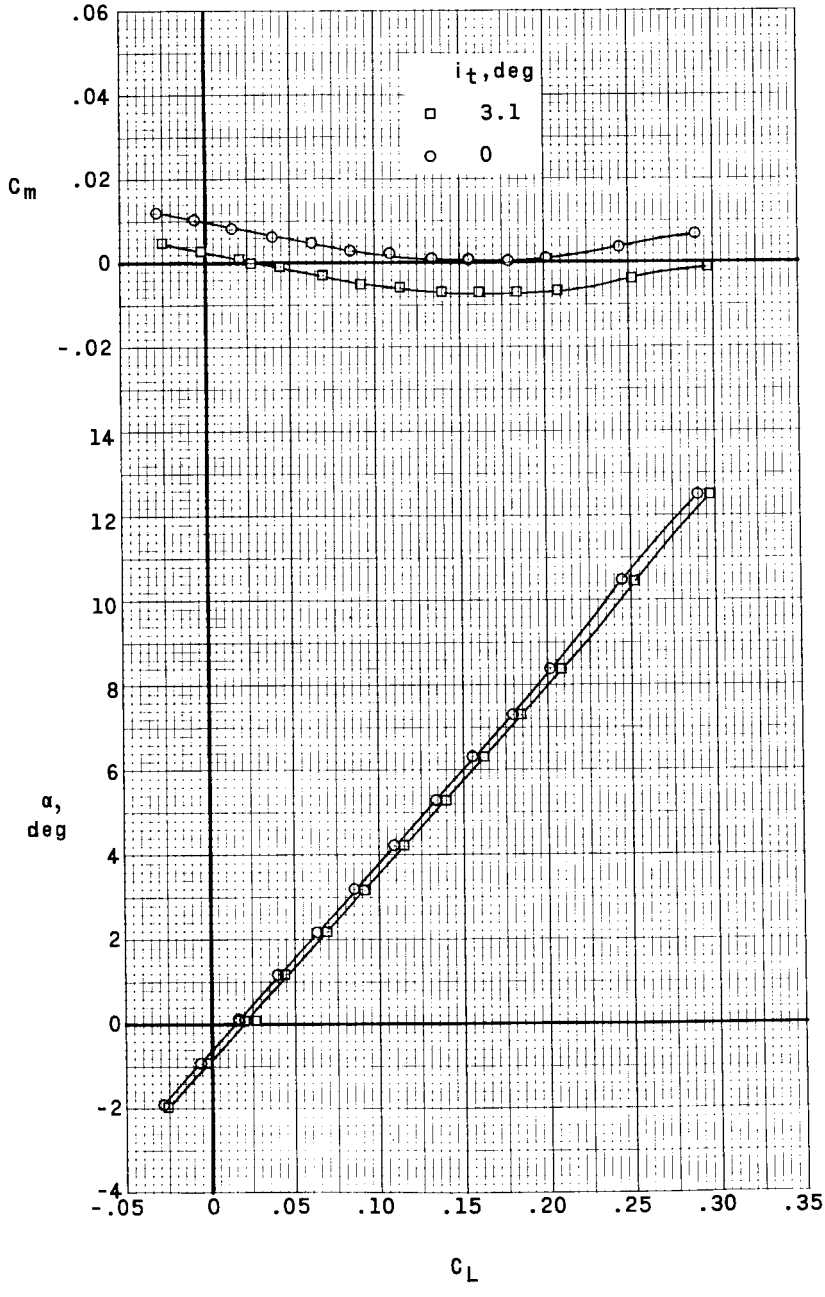

(d) M = 4.06.

Figure 7.- Continued.

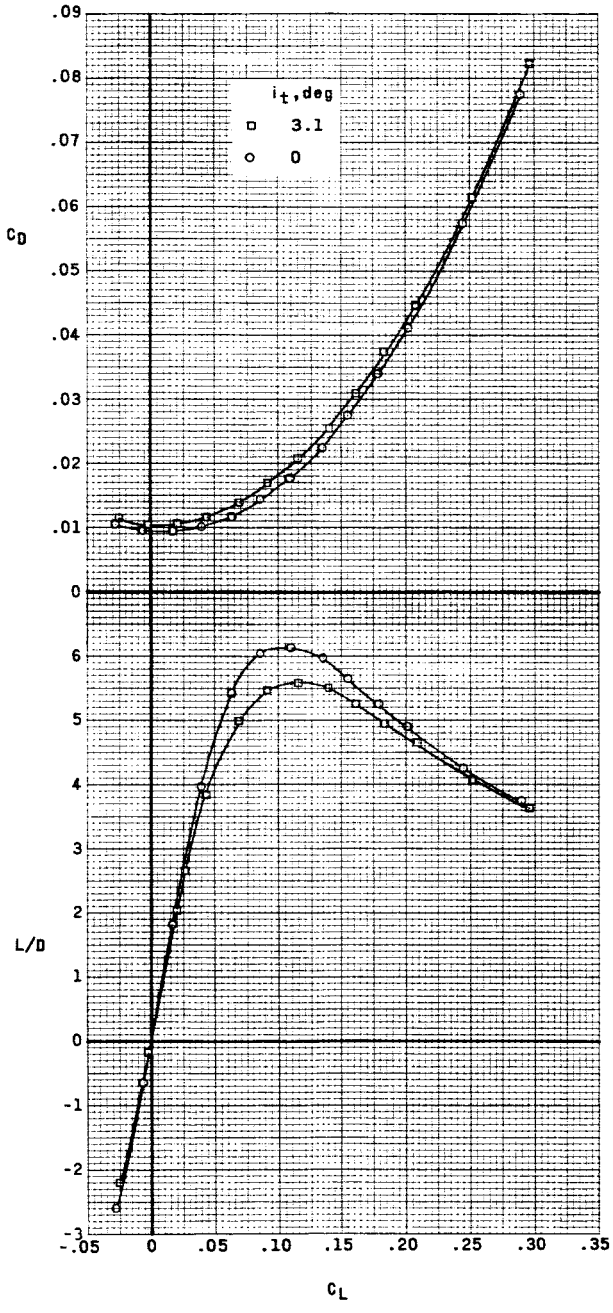

(d) M = 4.06. Concluded.

Figure 7.- Concluded.

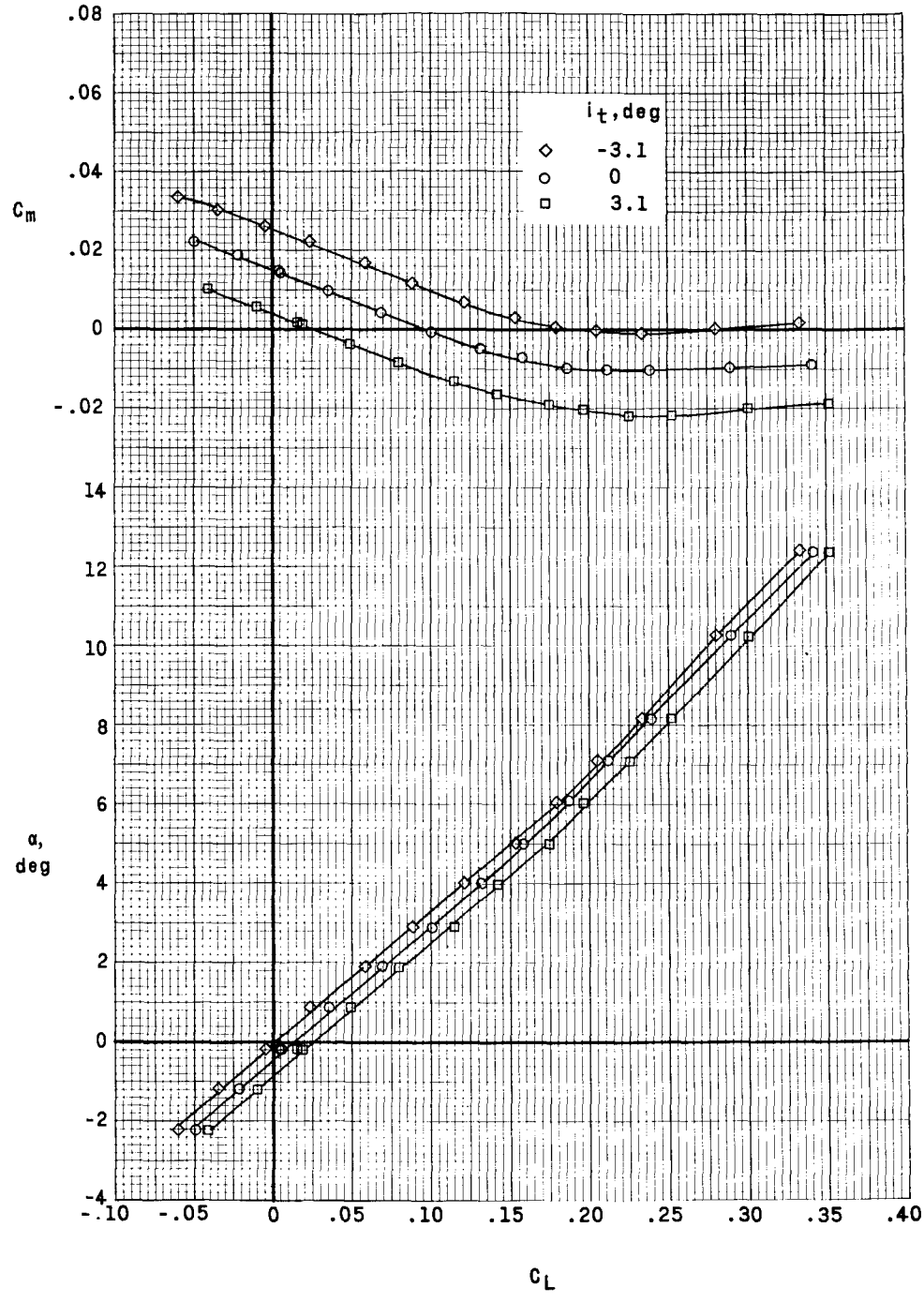

(a) M = 2.97.

Figure 8.- Effect of tail incidence on aerodynamic characteristics in pitch of the model with the large tail. (Coefficients are based on geometry of wing and large tail.)

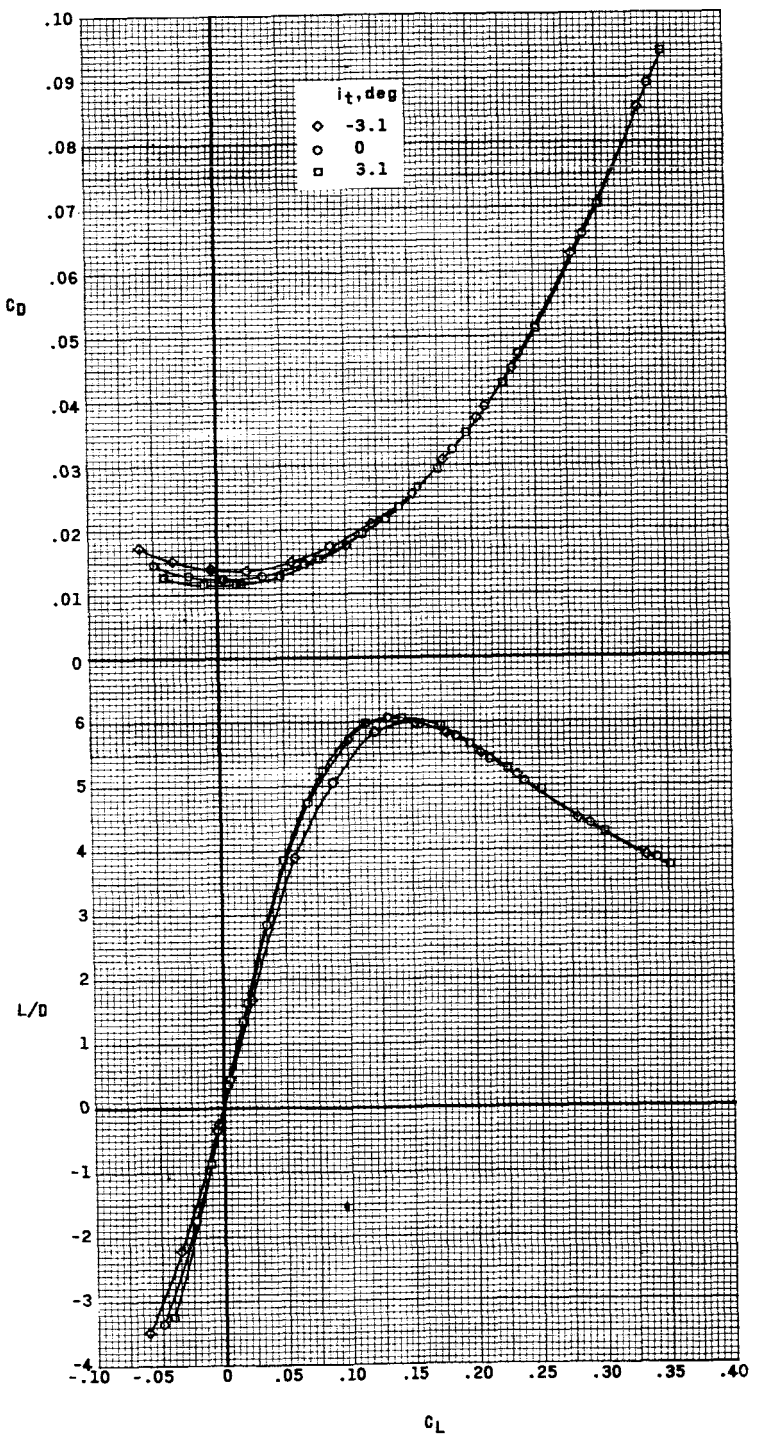

(a) M = 2.97. Concluded.

Figure 8.- Continued.

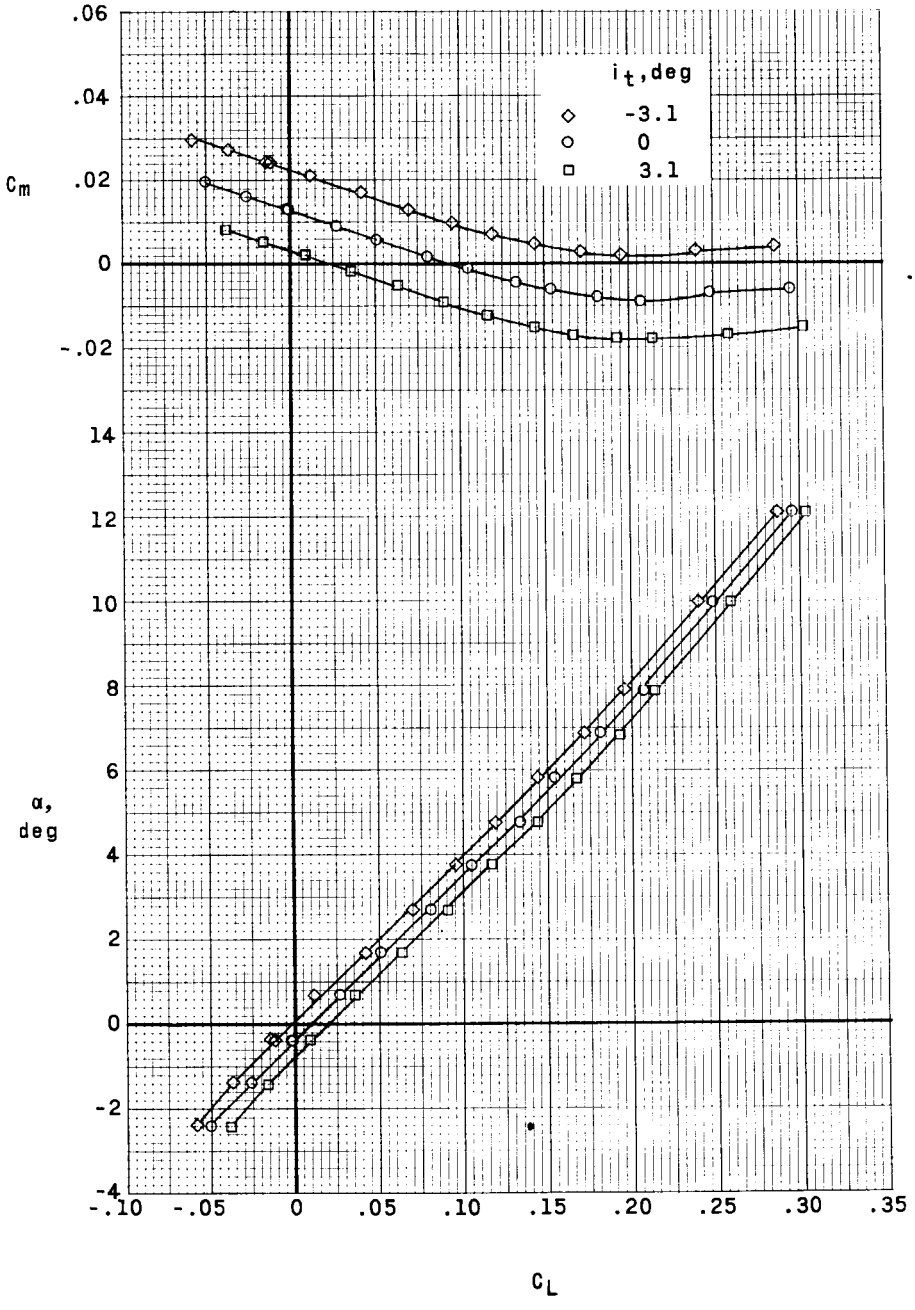

(b) M = 3.51.

Figure 8.- Continued.

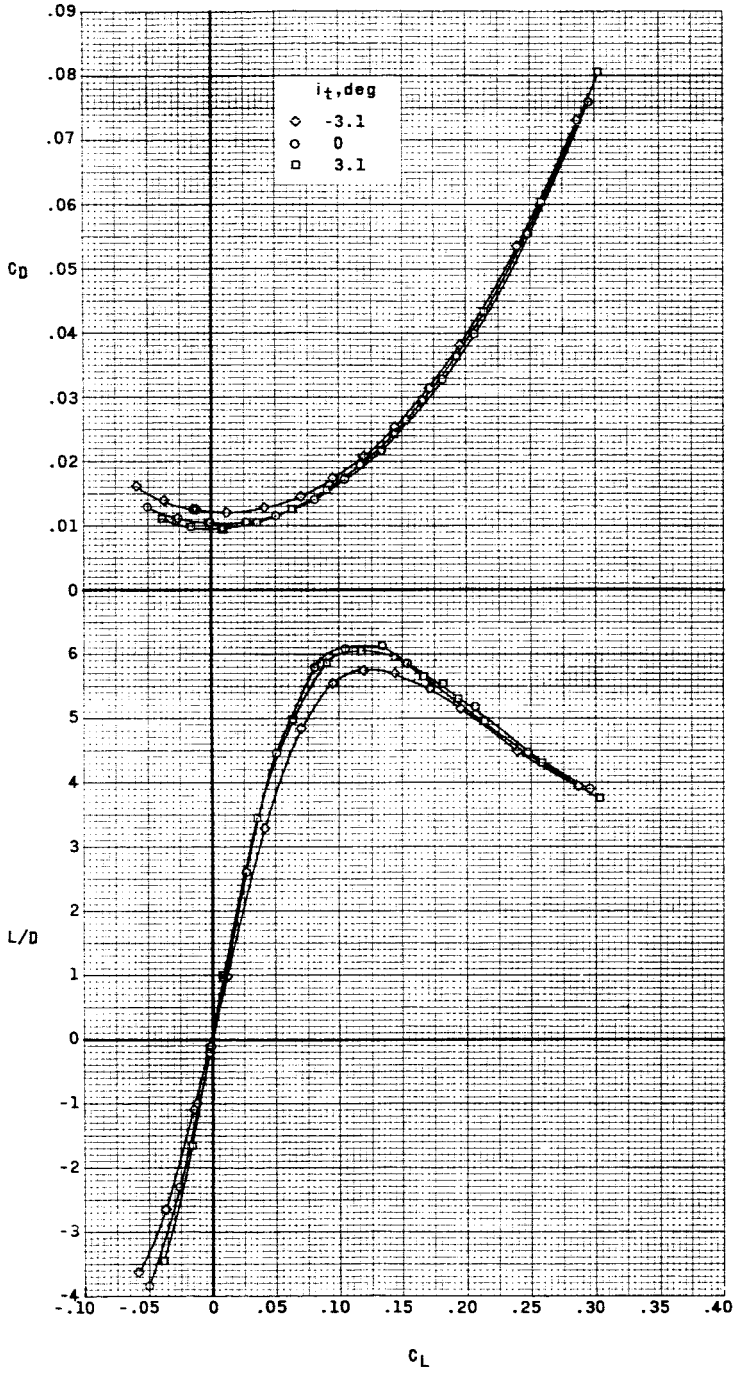

(b) M = 3.51. Concluded.

Figure 8.- Concluded.

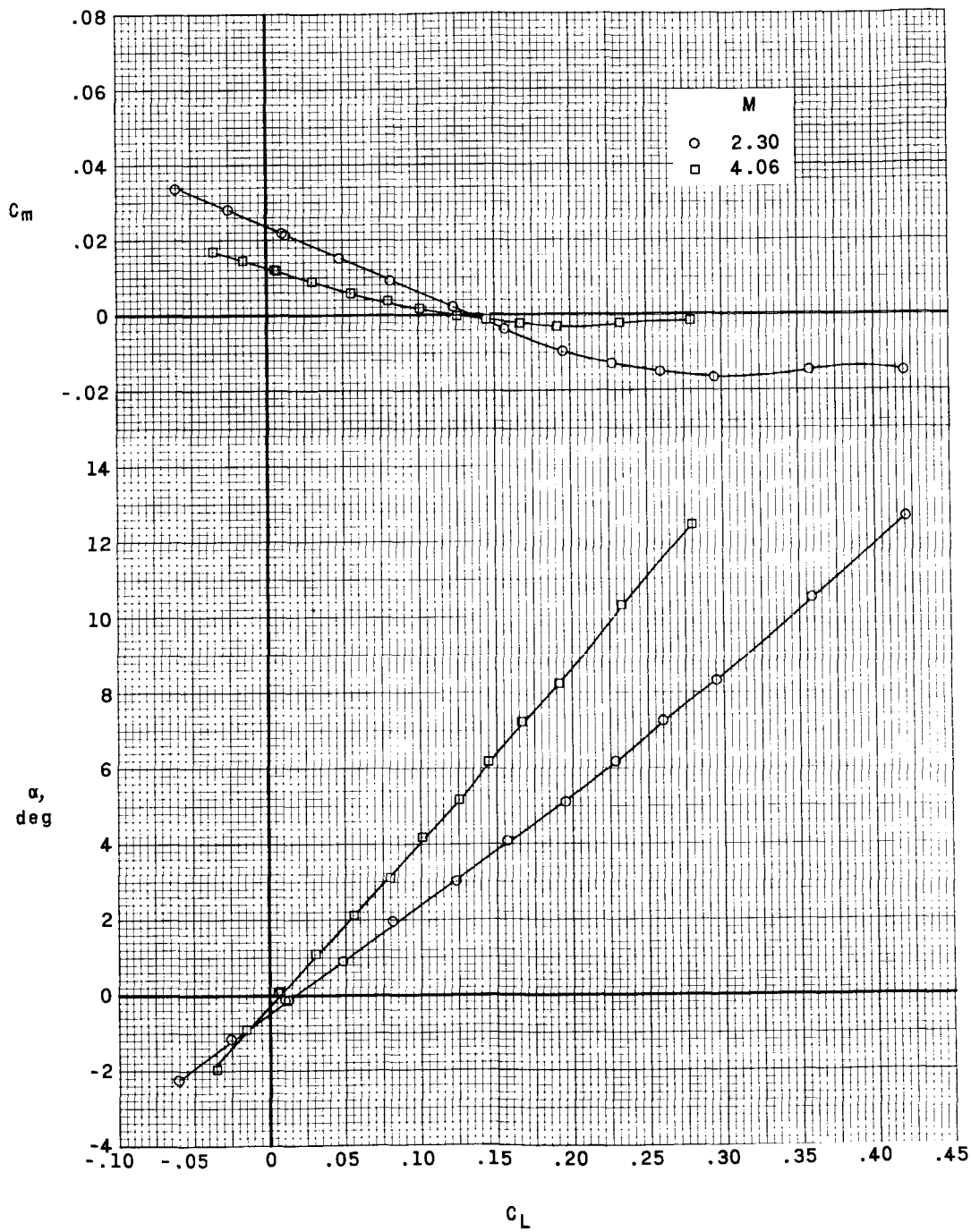

Figure 9.- Aerodynamic characteristics in pitch of the model with the large tail at M = 2.30 and M = 4.06 with $i_t = 0^o$. (Coefficients are based on geometry of wing and large tail.)

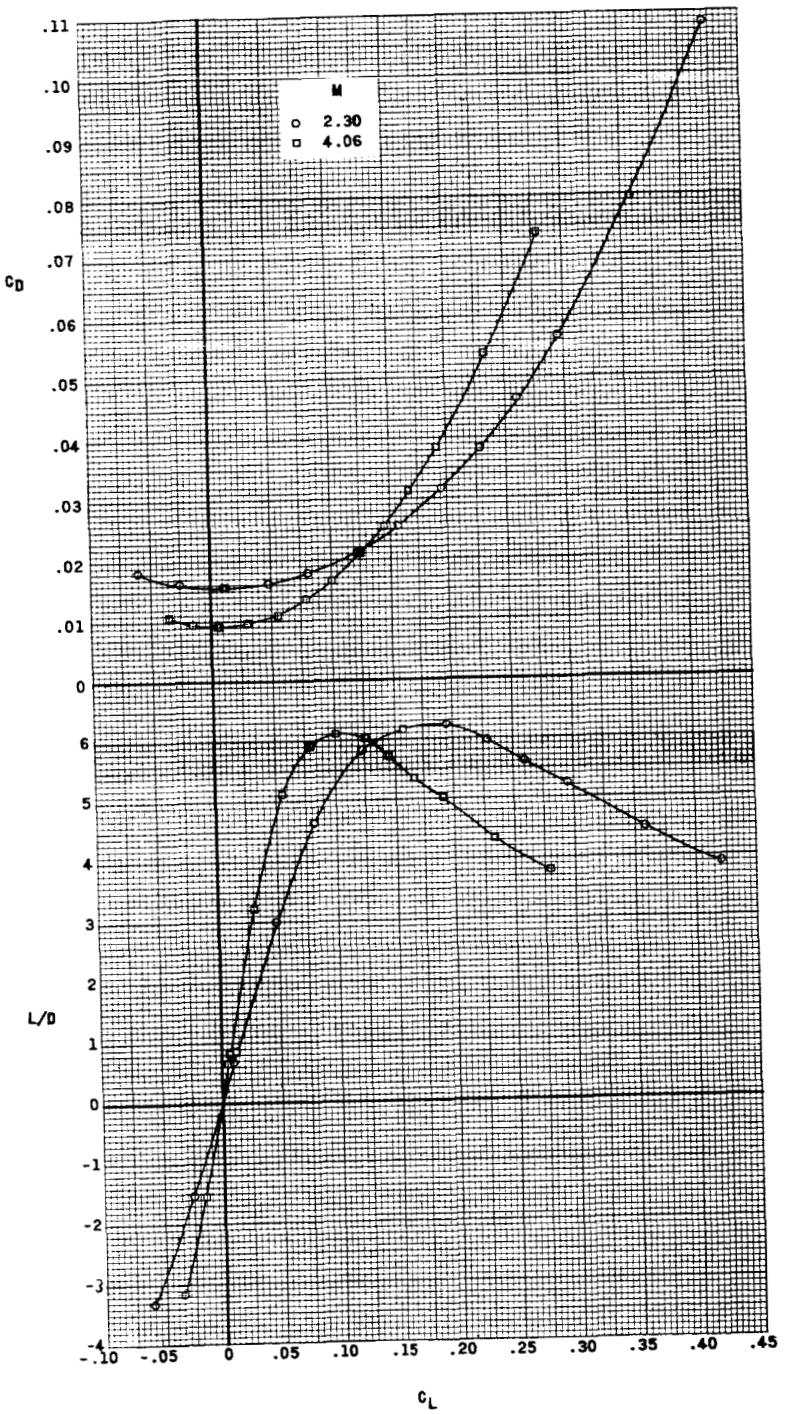

Figure 9.- Concluded.

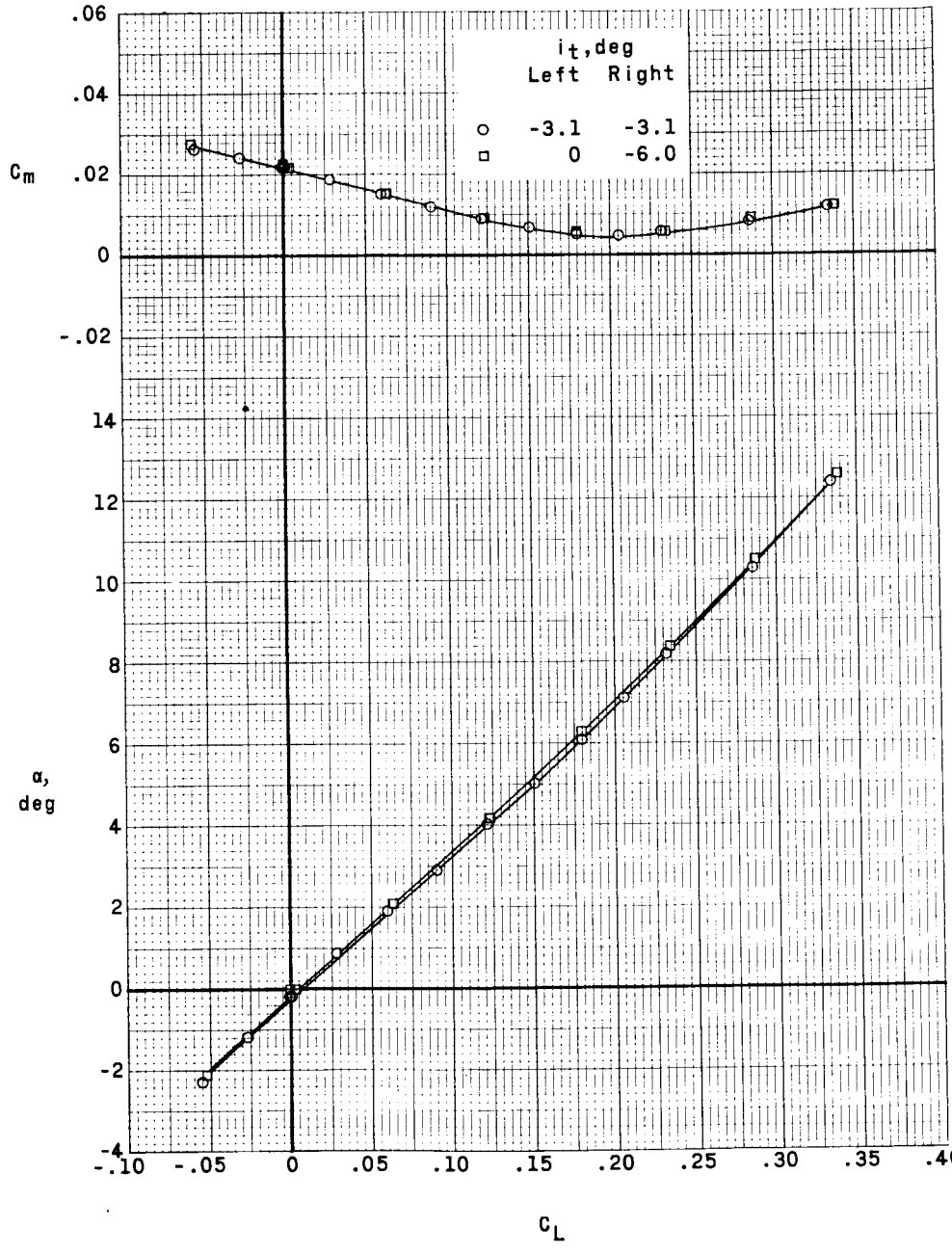

(a) Longitudinal characteristics.

Figure 10.- Effects of differential deflection of the basic horizontal tails when used as a roll control. M = 2.97; β = 0°.

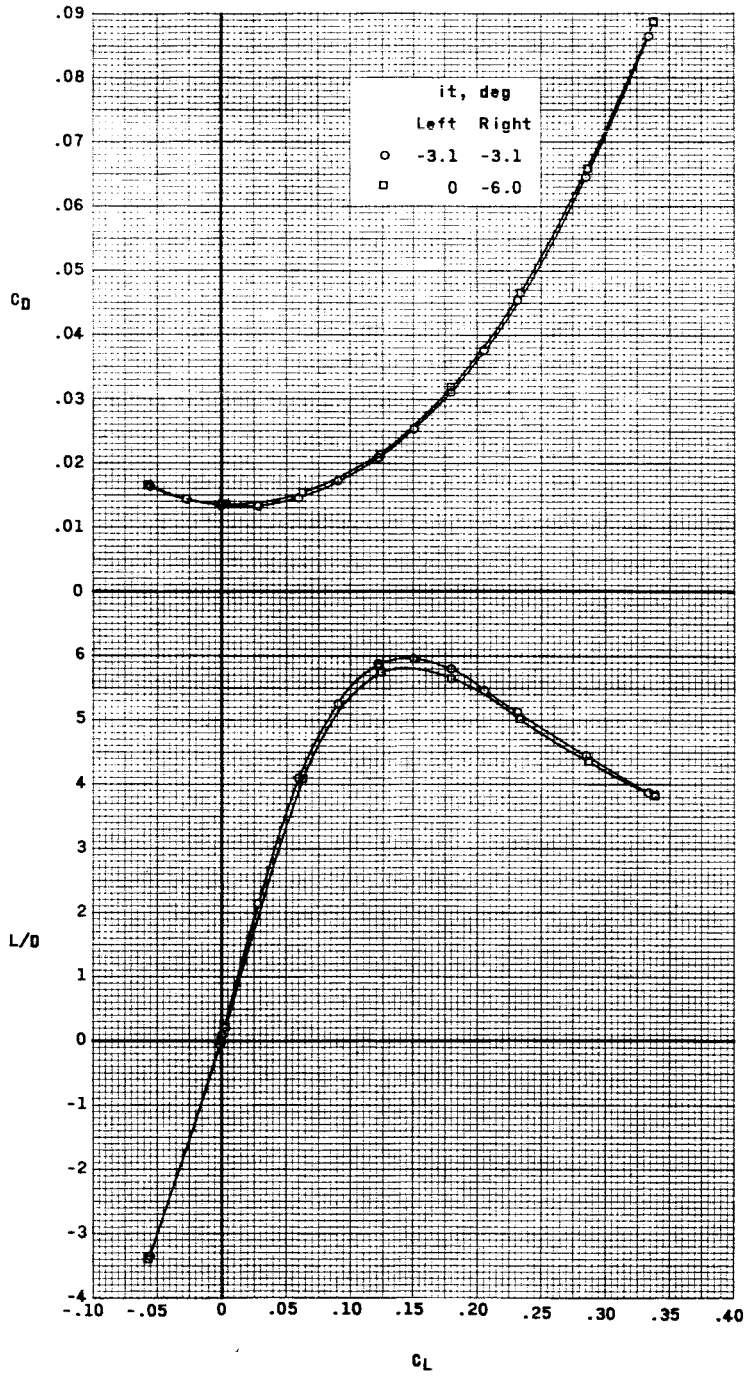

(a) Concluded.

Figure 10.- Continued.

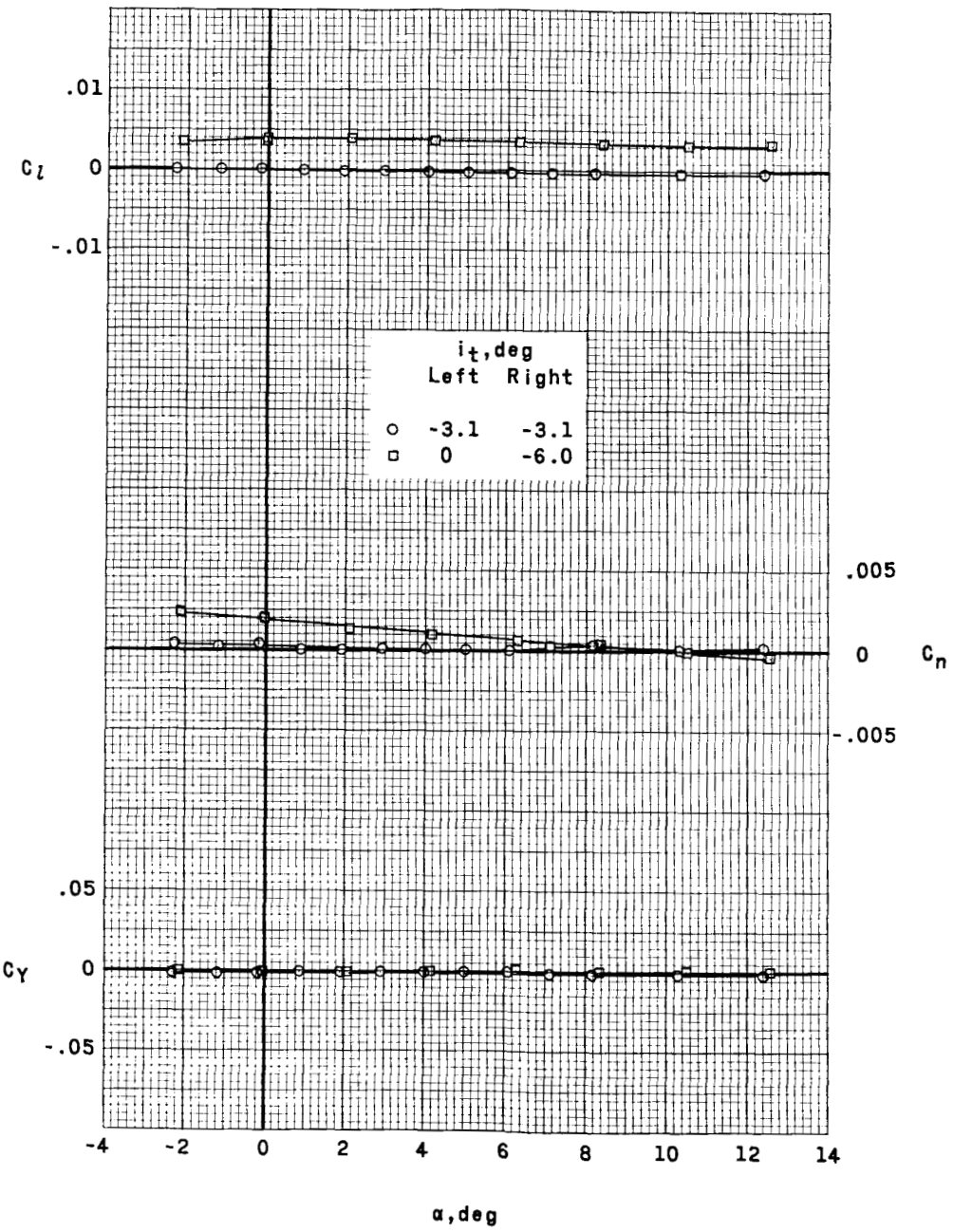

(b) Lateral characteristics.

Figure 10.- Concluded.

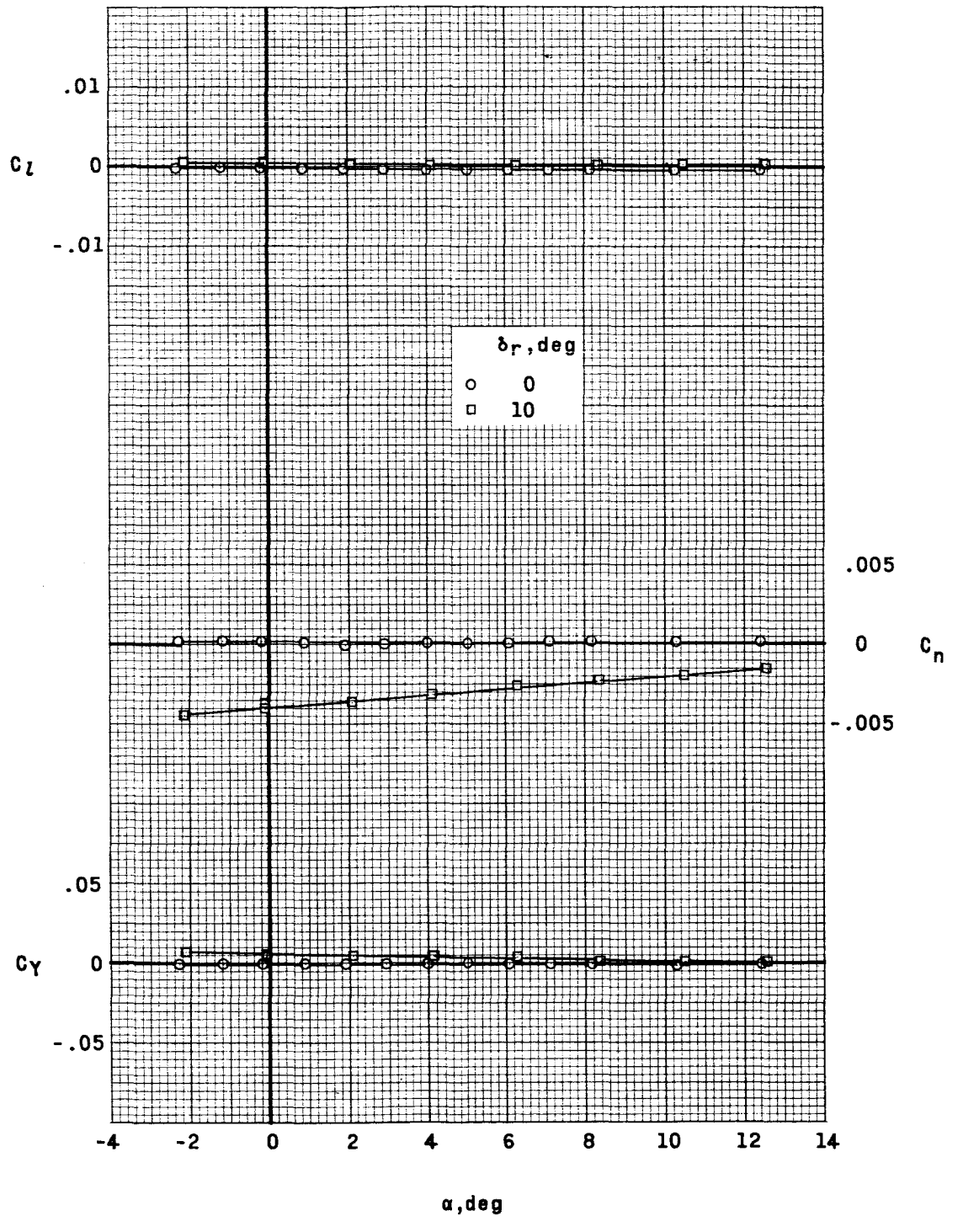

L-469

Figure 11.- Effect of rudder deflection at 0° sideslip for the basic model. M = 2.97.

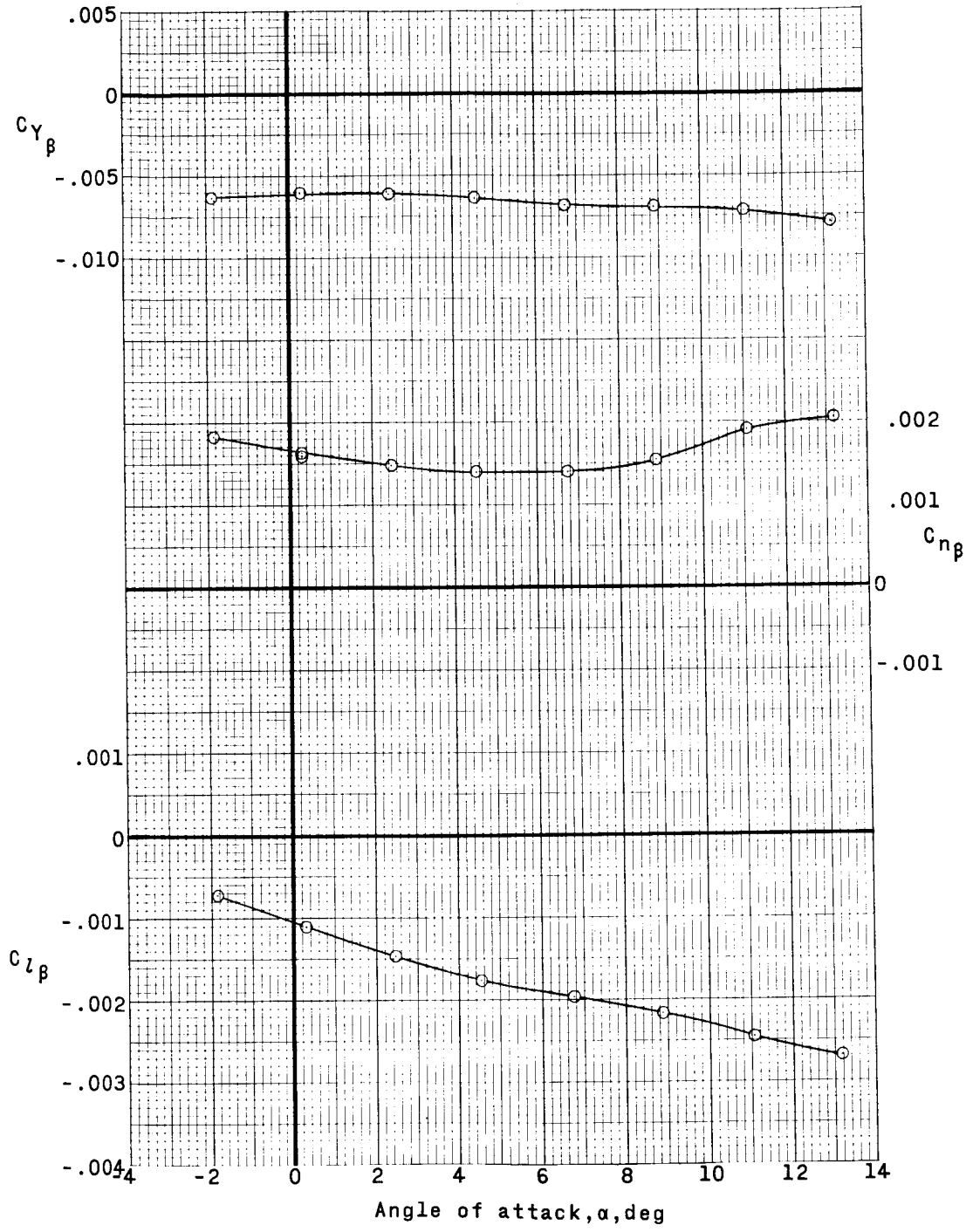

(a) M = 2.30.

Figure 12.- Lateral stability derivatives of the basic model.

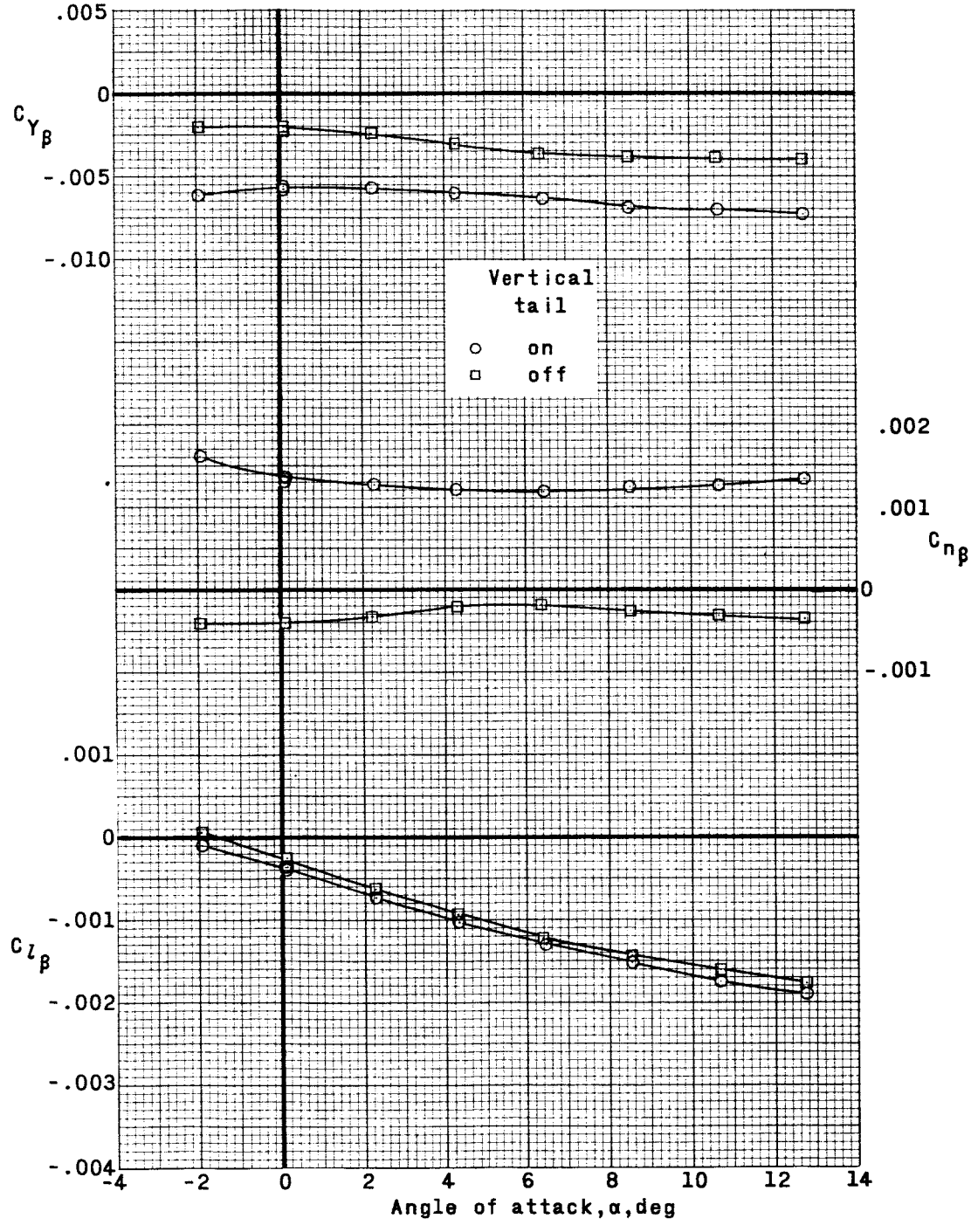

(b) M = 2.97.

Figure 12.- Continued.

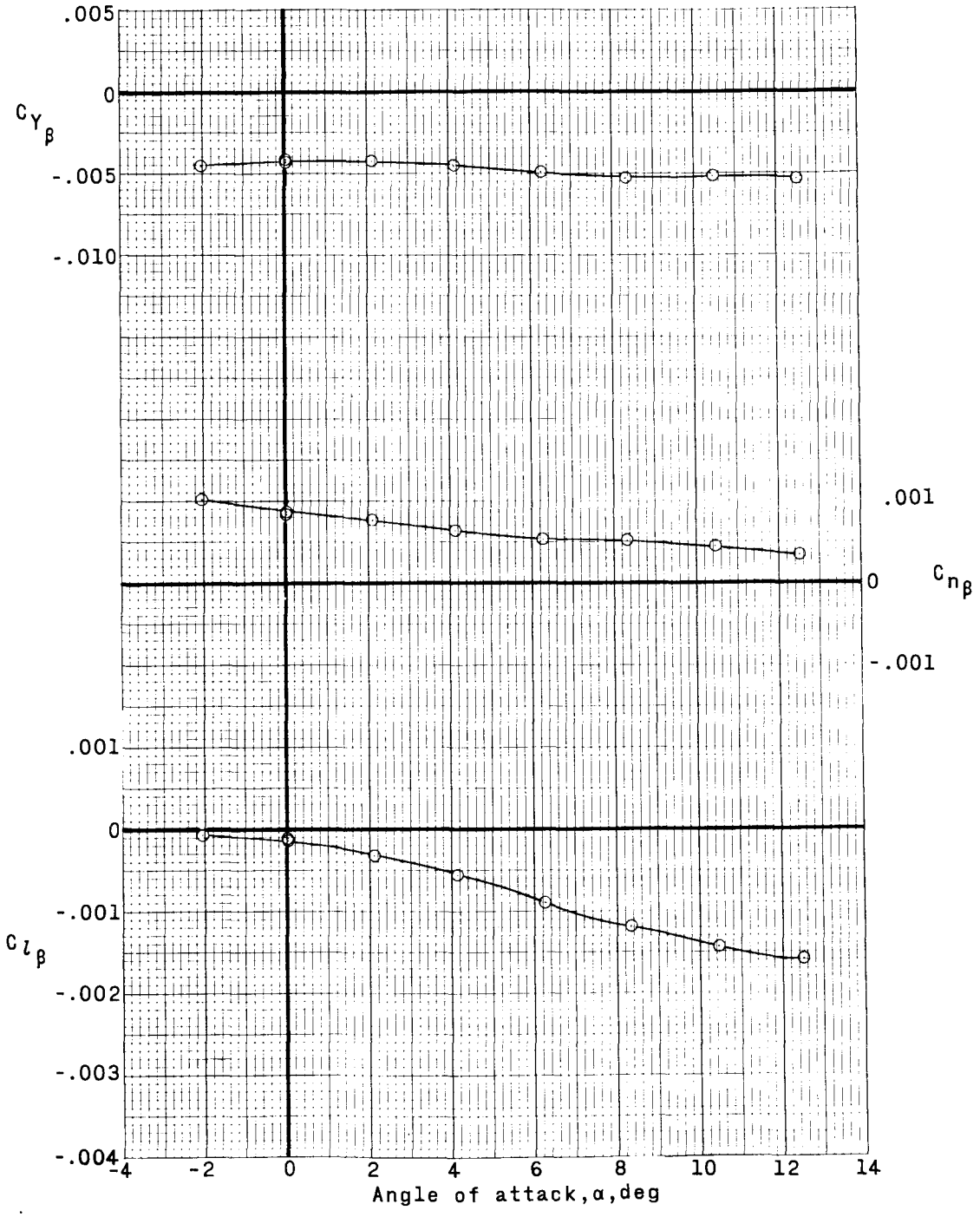

(c) M = 3.51.

Figure 12.- Continued.

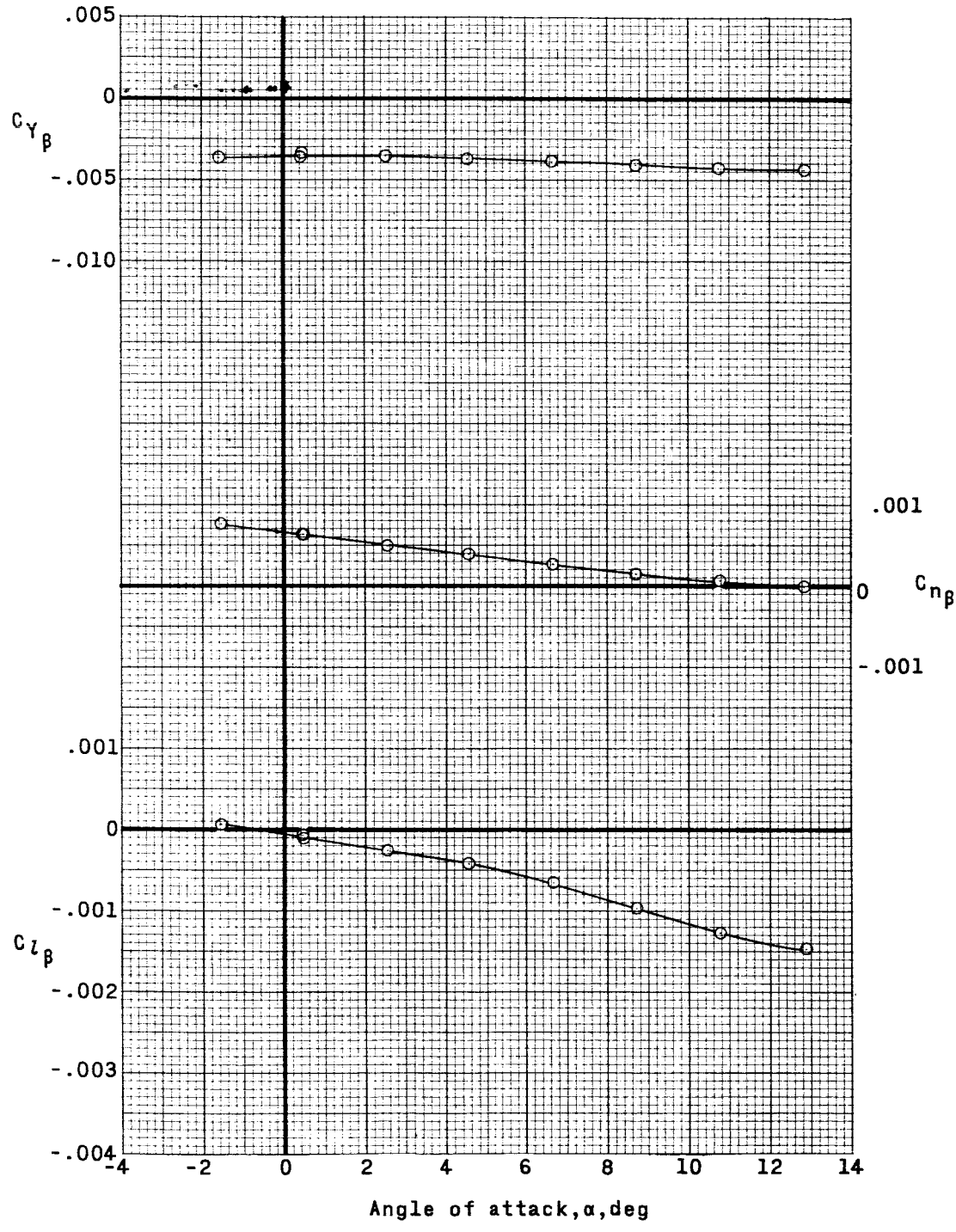

(d) M = 4.06.

Figure 12.- Concluded.

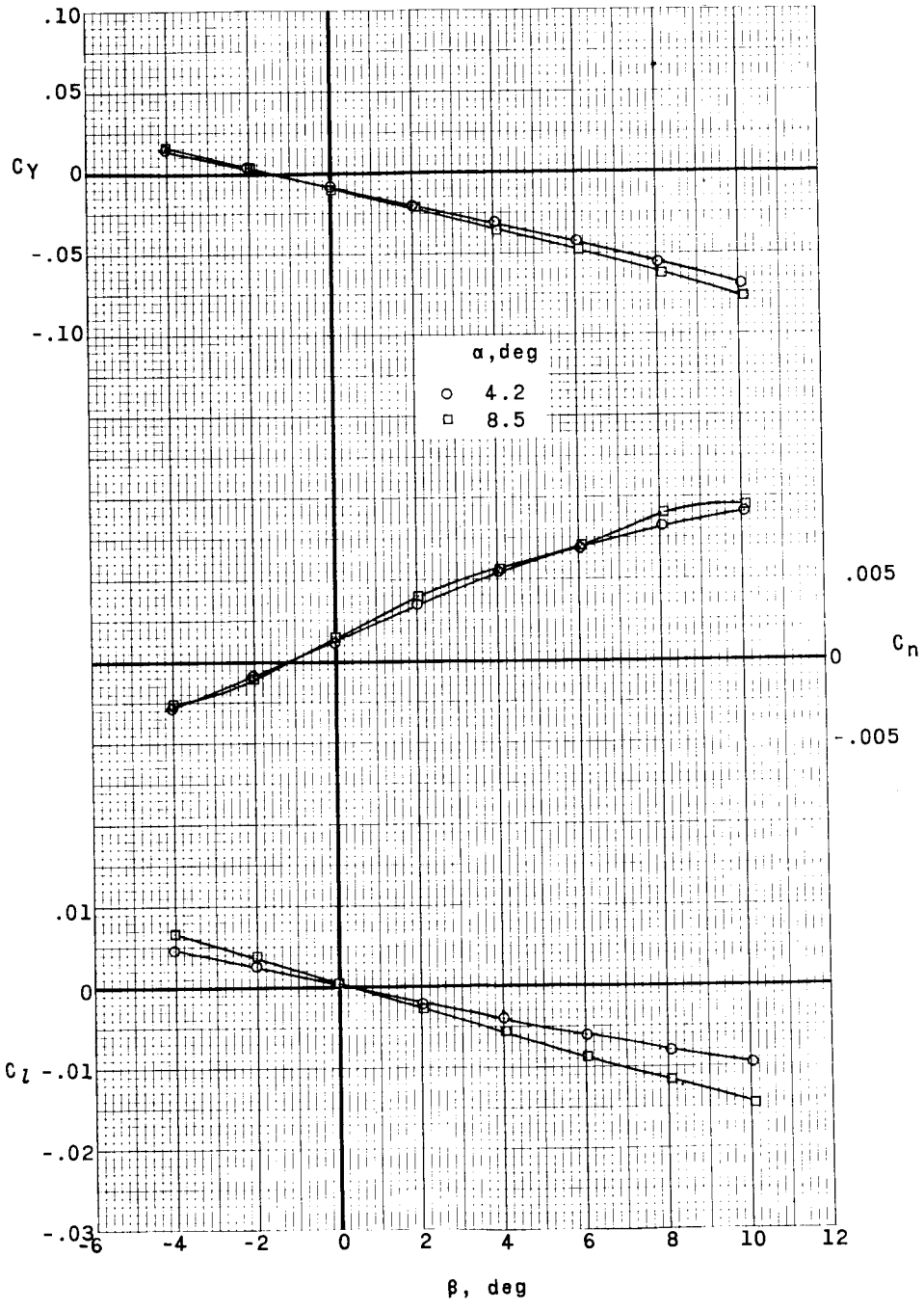

(a) Lateral characteristics.

Figure 13.- Aerodynamic characteristics in sideslip of the model with the basic horizontal tail. M = 2.97.

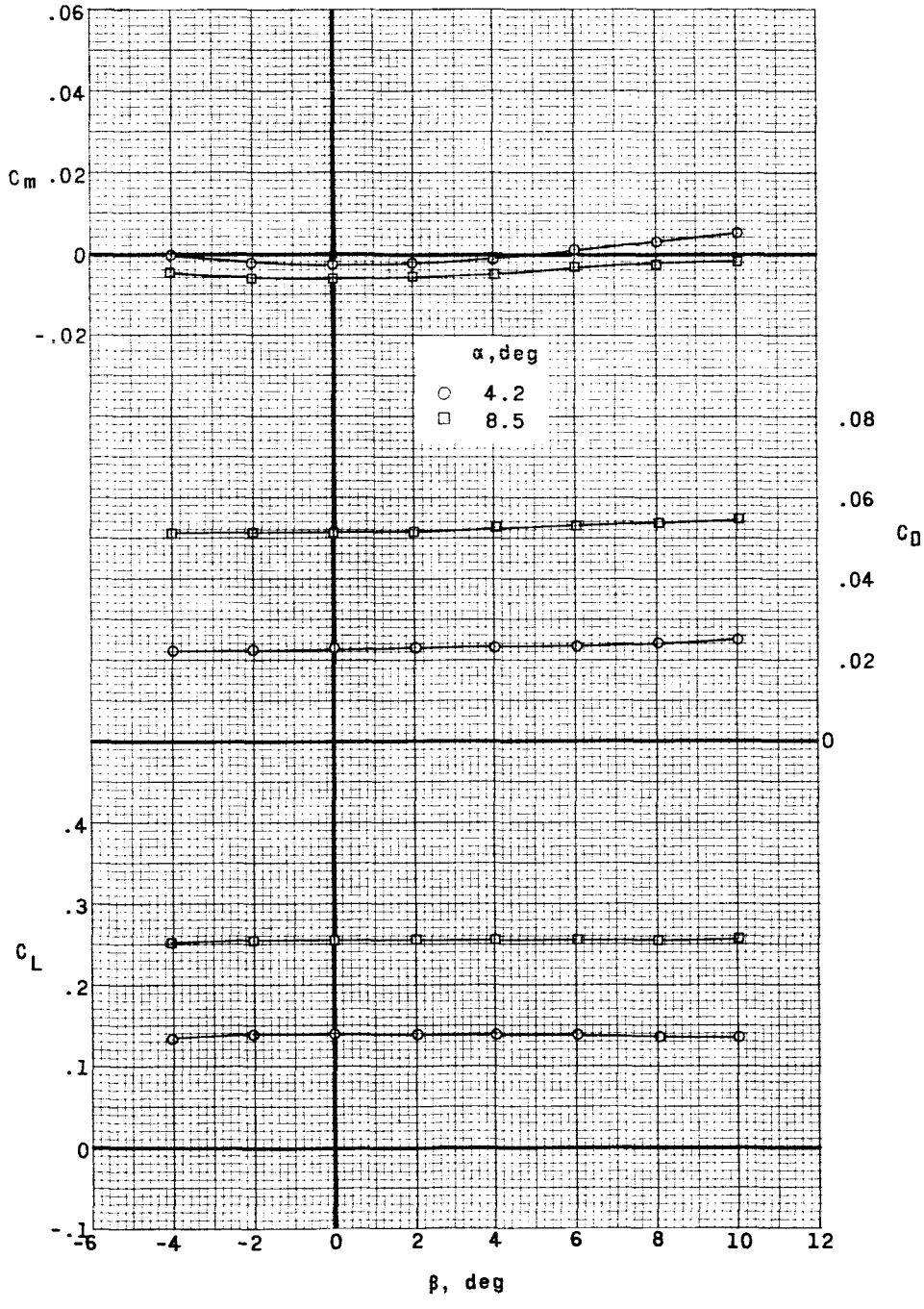

(b) Longitudinal characteristics.

Figure 13.- Concluded.

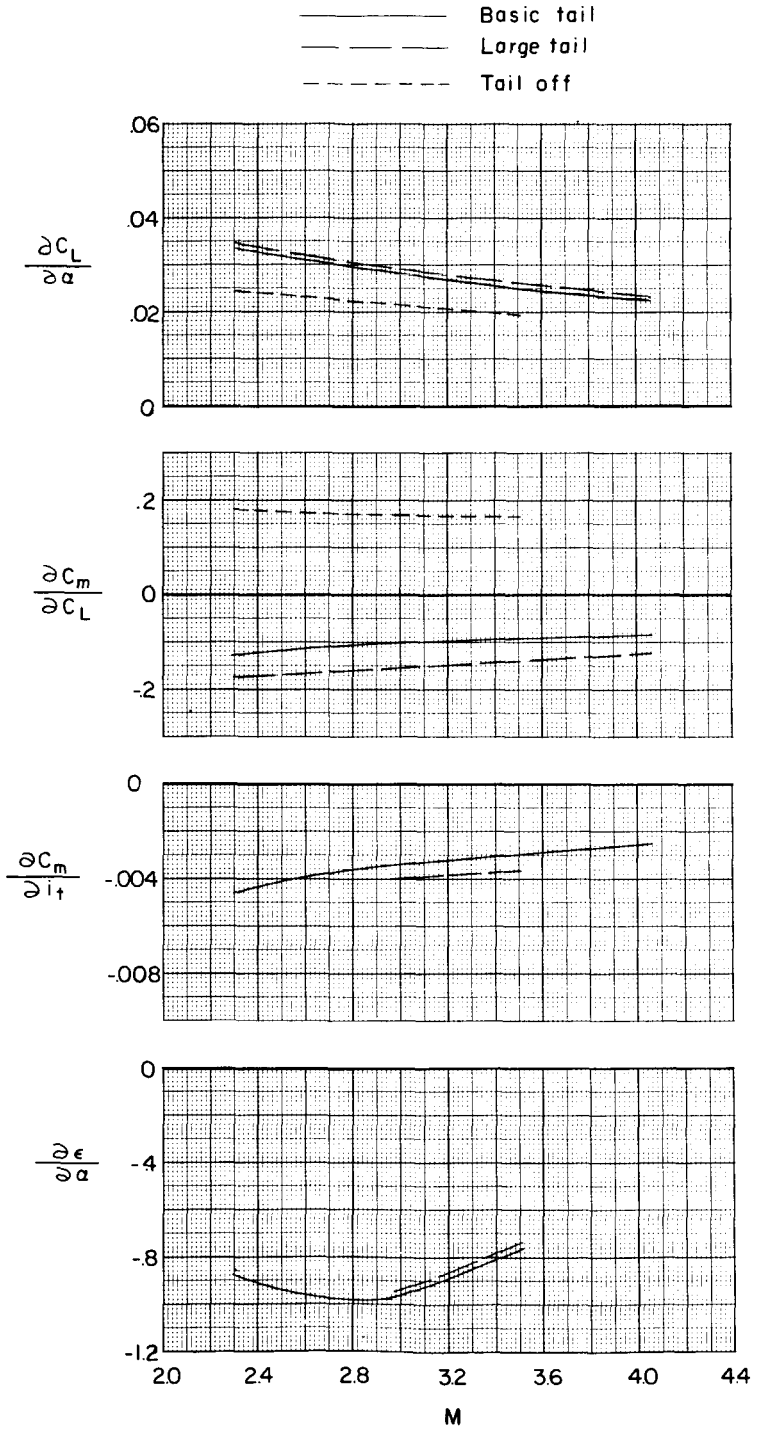

Figure 14.- Summary of the variation with Mach number of longitudinal stability parameters at low lift coefficients with $i_t = 0^\circ$ for tail-on configurations.

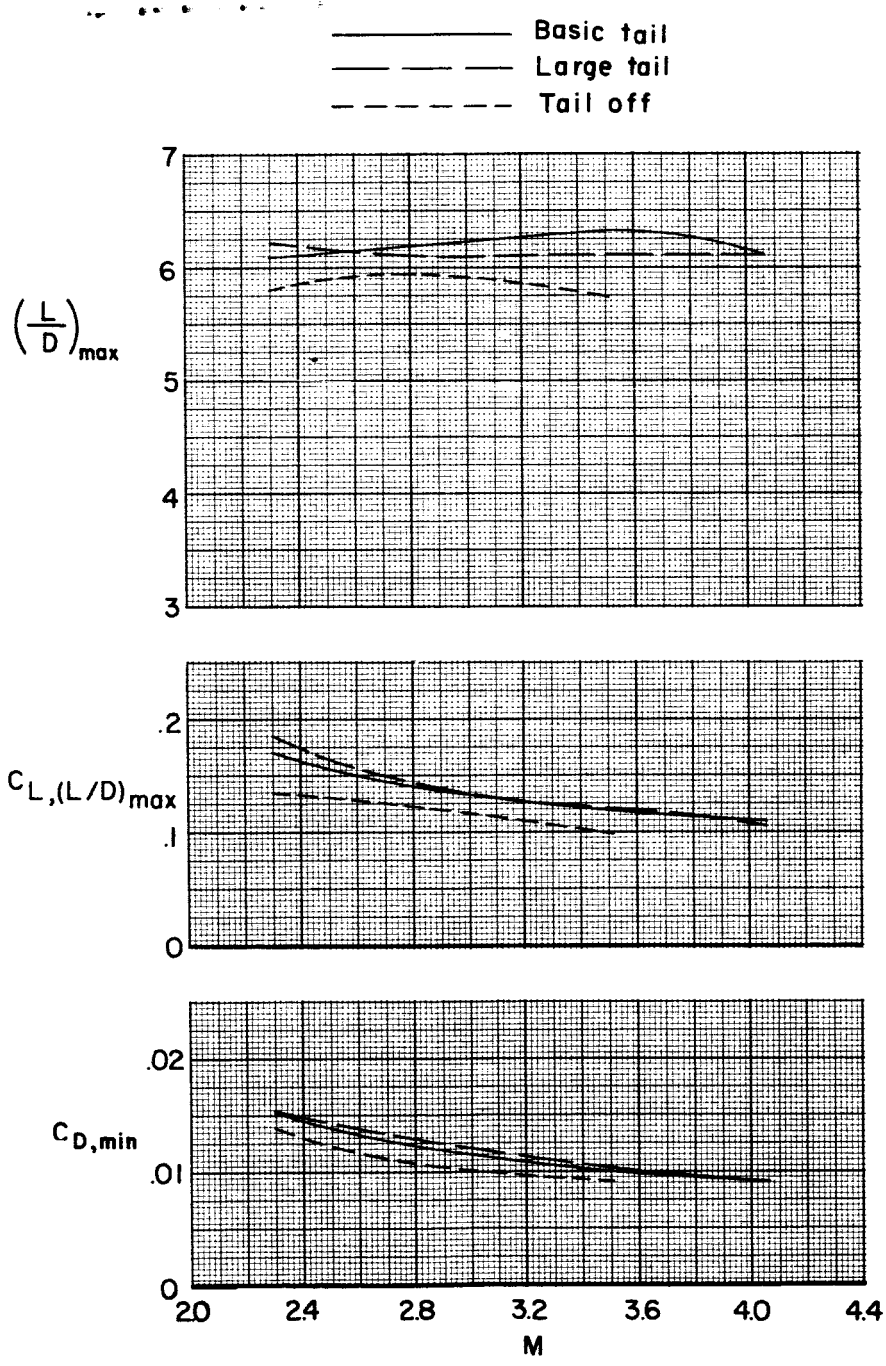

Figure 15.- Variation with Mach number of maximum lift-drag ratio, of lift coefficient for maximum lift-drag ratio, and of minimum drag coefficient with $i_t = 0^\circ$ for tail-on configurations.

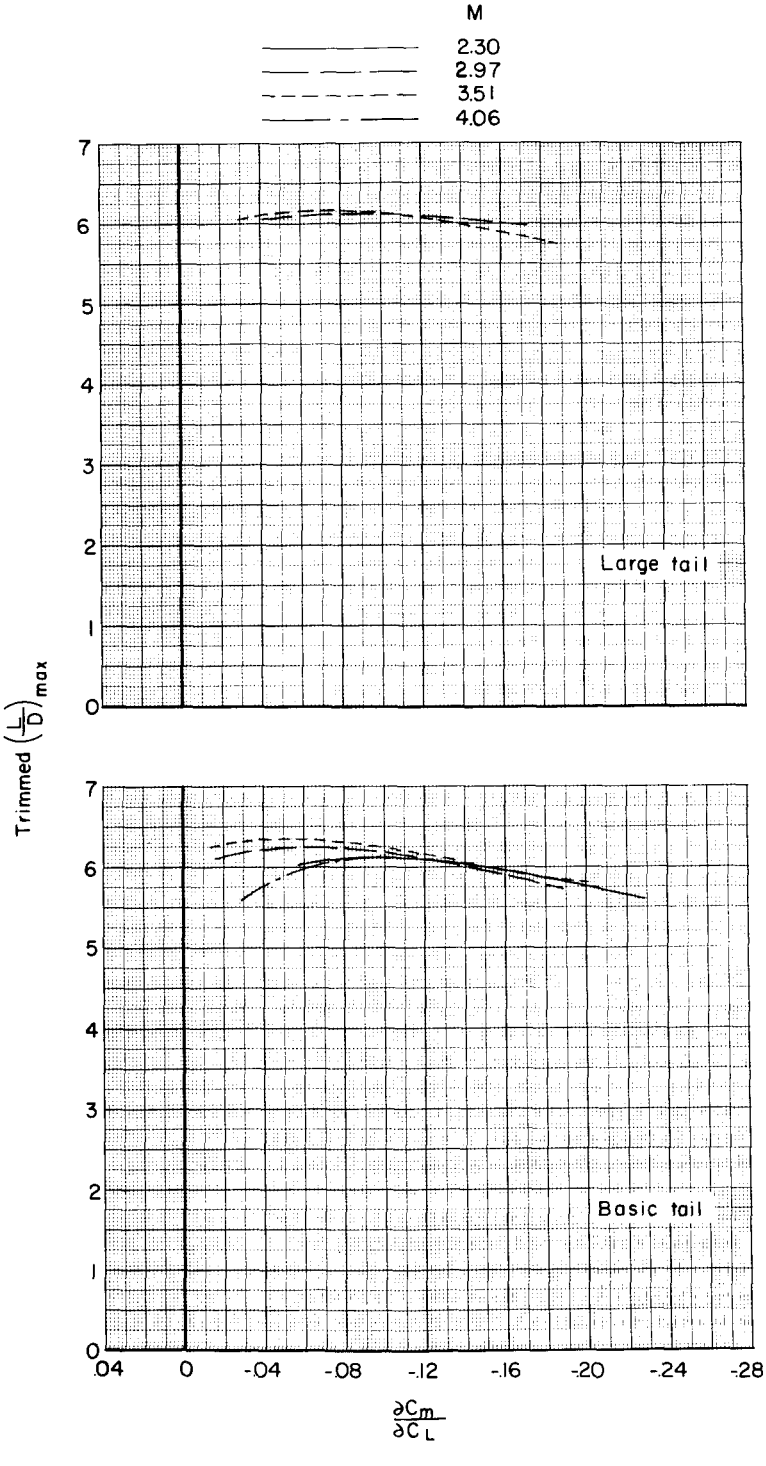

Figure 16.- Effect of the amount of static longitudinal stability at low lift on the maximum values of lift-drag ratio for trimmed conditions.

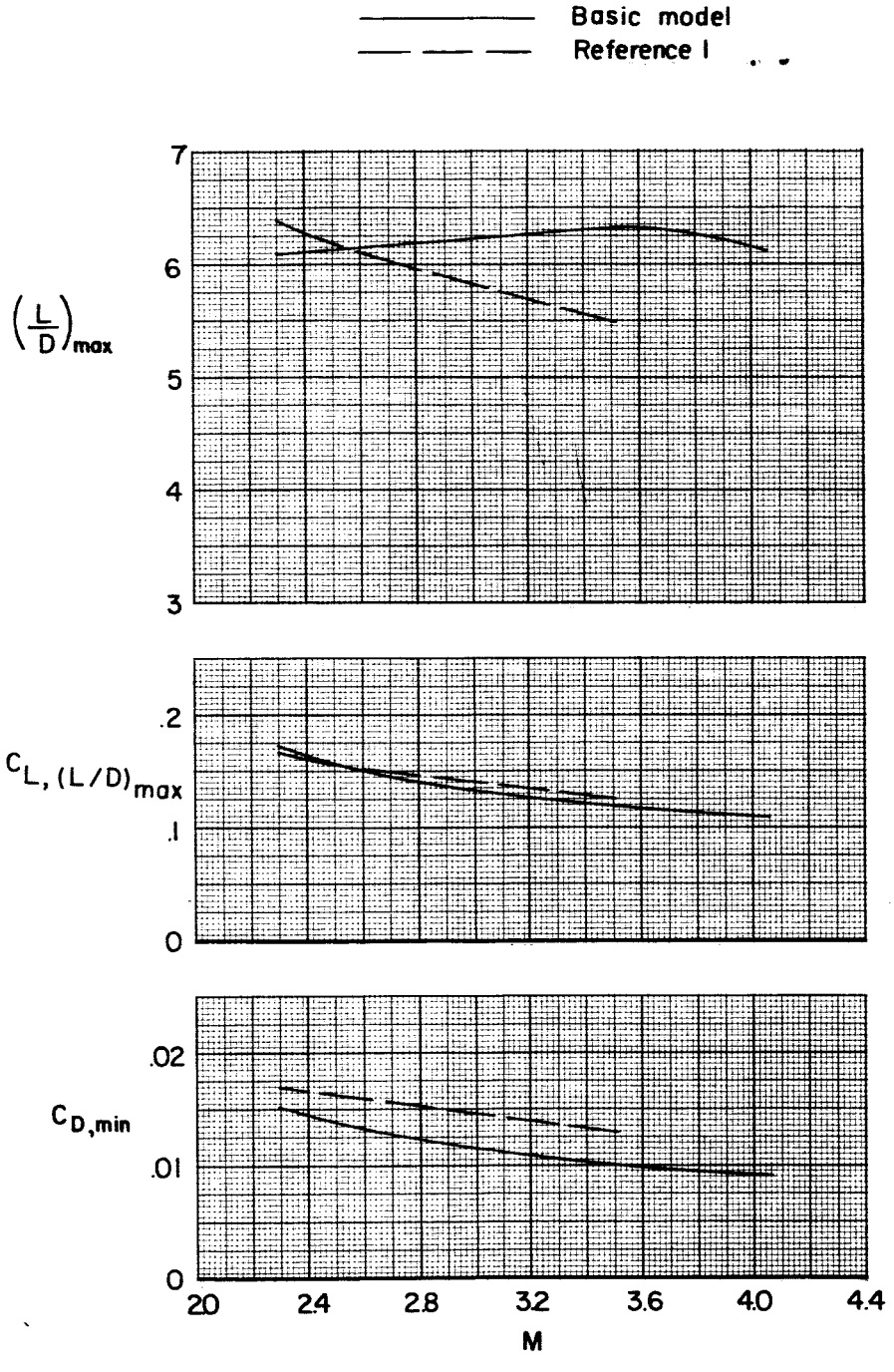

Figure 17.- Comparison between some performance parameters for the basic model with $i_t = 0^\circ$ and those for the outboard-tail model of reference 1 with $i_t = -0.1^\circ$.

NASA - Langley Field, Va. L-469